TECHNISCHE UNIVERSITÄT WIEN

Diploma Thesis

Microfluidic Spheroid Array for the Transport of Living Cell Cultures

submitted at TU Wien

Faculty of Technical Chemistry

Cell Chip Group

under the supervision of

Univ.Prof. Dipl.-Ing. Dr.Peter Ertl

M.Sc. Florian Selinger

by

Marzieh Keykhaei

52009245

Place and Date

Signature

Declaration of Authorship

I declare in lieu of oath, that I wrote this thesis and carried out the associated research myself, using only the literature cited in this volume. If text passages from sources are used literally, they are marked as such.

I confirm that this work is original and has not been submitted for examination elsewhere, nor is it currently under consideration for a thesis elsewhere.

I acknowledge that the submitted work will be checked electronically-technically using suitable and state-of-the-art means (plagiarism detection software). On the one hand, this ensures that the submitted work was prepared according to the high-quality standards within the applicable rules to ensure good scientific practice "Code of Conduct" at the TU Wien. On the other hand, a comparison with other student theses avoids violations of my personal copyright.

Place and Date

Signature

Acknowledgements

I would like to extend my sincere gratitude to Prof. Dr. Peter Ertl for granting me the opportunity to undertake my master's thesis within his esteemed research group.

My sincere thanks also go to all members of the Cell Chip group at TU Wien for their encouragement and fostering a collaborative and welcoming lab environment.

I am profoundly grateful to M.Sc. Florian Selinger for his exceptional supervision and guidance throughout this project. His profound expertise, thoughtful feedback, and consistent support were pivotal in addressing challenges and ensuring the successful completion of this work.

I also would like to acknowledge Univ. Ass. Dr. Martin Frauenlob and Univ. Ass. Dr. Silvia Schobesberger for their exceptional approachability and openness.

I am deeply grateful to my family and friends, especially my parents, for their love, support, and belief in me, which have given me strength and motivation.

I extend my heartfelt thanks to my husband, Dr. med. univ. Alireza Keykhaei. He celebrated my achievements, stood by me through challenges, and believed in me even in moments of doubt, which became the cornerstone of my journey.

Finally, I extend my sincere gratitude to everyone who contributed to the successful completion of this thesis.

"There is no greater wealth than wisdom, and no greater poverty than ignorance."

Ali ibn Abi Talib

List of Content

List of Figures

List of Abbreviations and Symbols

2D	Two dimensional
3D	Three dimensional
A549	Human lung adenocarcinoma epithelial cell line
AB	Antibiotic/antimycotic solution
CAD	Computer-Aided Design
Caco2	Human colorectal adenocarcinoma cell line
CBC	Cyclic Block Copolymer
CO_2	Carbon Dioxide
COC	Cyclic Olefin Copolymer
COP	Cyclic Olefin Polymer
CryoSOfree	CryoSOfree DMSO-free cryopreservation medium
DMEM	Dulbecco's Modified Eagle Medium
DMSO	Dimethyl sulfoxide
ECM	Extracellular matrix
FBS	Fetal bovine serum
HA	Hyaluronic acid
HEK	Human Embryonic Kidney 293
HeLa	Henrietta Lacks' cell
HepG2 C3A	Subclone of HepG2 human hepatocellular carcinoma cell line
Hoechst	Hoechst H33342
HSPs	Heat shock proteins
MDCK	Madin-Darby Canine Kidney cells
MEM	Minimum Essential Medium
Nutrifreez	Nutrifreez D10 cryopreservation medium
PDMS	Polydimethylsiloxane
PI	Polyimide
PMMA	Poly Methyl Methacrylate
PS	Polystyrene
PVC	Polyvinyl Chloride
SH-SY5Y	Subclone of human neuroblastoma cell line SK-N-SH

Abstract

Efficient transportation and storage of live cells are vital for progress in regenerative medicine, cell banking, and therapeutic development. Current cell transportation methods face notable challenges: transporting cryopreserved cells with liquid nitrogen is expensive and hazardous, while dry ice risks evaporation and exacerbates dimethyl sulfoxide (DMSO) toxicity. Meanwhile, live-cell transport in culture media is hindered by oxygen depletion and pH instability. These limitations underscore the critical need for more reliable and effective methods.

Spheroids, as a form of 3D cell culture, offer a promising alternative due to their structural and functional similarity to native tissues, as well as their enhanced resilience to the stresses of cryopreservation and transportation compared to traditional 2D cultures and single-cell suspensions. To integrate these advantages into a practical workflow, various buffer systems and cryoprotectant formulations were tested in HEK and HeLa cell lines to evaluate their effectiveness in supporting spheroid formation, cryopreservation, and recovery. Results indicated that CO_2-independent media combined with NutriFreez cryoprotectant solutions yielded higher post-thaw viability compared to other tested conditions. HeLa spheroids demonstrated the best viability and successful reculturing after thawing, while HEK spheroids exhibited reduced viability, emphasizing the need for cell-line-specific optimization.

A novel 3D-printed Cryoinsert prototype was developed to further support this workflow by facilitating spheroid formation and freezing during transportation. While the device effectively maintained spheroid structural integrity, post-thaw viability was compromised by resin-derived toxins. Enhancing the biocompatibility of the Cryoinsert material, along with optimizing cryopreservation protocols, is essential for addressing these challenges and providing a reliable solution for the transportation of live cells.

Zusammenfassung

Effizienter Transport und die Lagerung lebender Zellen sind entscheidend für den Fortschritt in der regenerativen Medizin, Zellbanken und der therapeutischen Entwicklung. Aktuelle Methoden für den Zelltransport stehen vor erheblichen Herausforderungen: Der Transport kryokonservierter Zellen mit flüssigem Stickstoff ist teuer und gefährlich, während Trockeneis die Verdunstung und die Toxizität von Dimethylsulfoxid (DMSO) verstärken kann. Gleichzeitig wird der Transport lebender Zellen in Kulturmedien durch Sauerstoffmangel und pH-Instabilität beeinträchtigt. Diese Einschränkungen verdeutlichen den dringenden Bedarf an zuverlässigeren und effektiveren Methoden.

Sphäroide, als Form der 3D-Zellkultur, bieten eine vielversprechende Alternative, da sie in ihrer Struktur und Funktion nativen Geweben ähneln und widerstandsfähiger gegenüber den Belastungen durch Kryokonservierung und Transport sind als herkömmliche 2D-Kulturen und Einzelzell-Suspensionen. Um diese Vorteile in einen praktischen Workflow zu integrieren, wurden verschiedene Puffersysteme und Kryoprotektiva in HEK- und HeLa-Zelllinien getestet, um ihre Eignung zur Unterstützung von Sphäroidbildung, Kryokonservierung und Erholung zu bewerten. Die Ergebnisse zeigten, dass CO_2-unabhängige Medien in Kombination mit NutriFreez-Kryoprotektiva eine höhere Lebensfähigkeit nach dem Auftauen erzielten als andere getestete Bedingungen. HeLa-Sphäroide wiesen die beste Lebensfähigkeit und erfolgreiche Rekultivierung nach dem Auftauen auf, während HEK-Sphäroide eine geringere Lebensfähigkeit zeigten, was die Notwendigkeit einer zelllinienspezifischen Optimierung unterstreicht.

Ein neuartiger, 3D-gedruckter Cryoinsert-Prototyp wurde entwickelt, um diesen Workflow weiter zu unterstützen, indem er die Sphäroidbildung und das Einfrieren während des Transports erleichtert. Während das Gerät die strukturelle Integrität der Sphäroide effektiv aufrechterhielt, wurde die Lebensfähigkeit nach dem Auftauen durch harzbedingte Toxine beeinträchtigt. Die Verbesserung der Biokompatibilität des Cryoinsert-Materials sowie die Optimierung der Kryokonservierungsprotokolle sind entscheidend, um diese Herausforderungen zu bewältigen und eine zuverlässige Lösung für den Transport lebender Zellen zu schaffen.

1. Introduction

In biomedical research, effective experimental models need to be dependable, accurately reflect human conditions, and help us understand how cells and organs respond to different factors [1].

Cell culture techniques are widely used in research to understand cellular behavior and mechanisms. This field owes its origins to Ross Granville Harrison, who in 1907 developed a method to keep living cells in the lab, paving the way for *in vitro* cell culture studies. Following initial studies, researchers like Holtfreter, Moscona, and Leighton worked to improve *in vitro* cell culture techniques, leading to significant advancements in this field [2].

These advancements have made cell culture technology reliable, robust, and well-developed. As a result, many biotherapeutics are now produced using these methods in large-scale manufacturing facilities, providing products for both commercial use and clinical research [3, 4].

Animal cell cultures were crucial for lab research for many years, specifically the demand for human viral vaccines in the 1950s spurred the development of large-scale cell-growing methods [5, 6].

These methods required anchorage-dependent cells. Today, modern viral vaccine technology uses microcarrier systems in stirred tank bioreactors, allowing cells to grow efficiently in pseudo-suspension cultures. Recently, the focus on mammalian cell culture bioprocesses has increased due to recombinant protein technology advancements from the 1970s and 1980s. The first human therapeutic protein from this technology was recombinant insulin, licensed in 1982. It was soon realized that more complex recombinant therapeutics required the post-translational capabilities of eukaryotic cells. Currently, up to 400 licensed biopharmaceuticals are produced using mammalian cell processes, including recombinant proteins, monoclonal antibodies, and nucleic acid-based products. Since 1996, chimeric and humanized monoclonal antibodies, such as Rituxan, Remicade, Synagis, and Herceptin, have become dominant [6-8].

Progress in cell culture techniques includes the development of new methods and the enhancement of media supplements [9].

One significant advancement is the advent of 3D culture approaches, which have numerous applications such as drug discovery and pharmacological testing, tumor models and cancer biology, gene and protein expression studies, cell physiology research, cell proliferation and cell-cycle studies, cytoskeleton studies, apoptosis research, and cell adhesion and signaling investigations. The flexibility of *in vitro* cell culture systems allows for a wide range of experimental variations, making them invaluable tools in scientific research [9].

Isolating and maintaining specific cell types in culture is an essential tool in scientific research. It enables researchers to investigate and analyze complex molecular interactions within organs and tissues, which are often challenging or impossible to observe in intact organisms. These *in vitro* systems allow for precise experimental control. Primary cell cultures can be established by enzymatic dissociation or migration from tissue explants. However, these cells have limited proliferative abilities, but they can replicate extensively, leading to the creation of cell lines that can proliferate indefinitely from single cellular lineages [10].

As culturing cells and tissues is essential for conducting research in the life sciences, the capacity to exchange cells and tissue-engineered constructs with fellow researchers is crucial [11].

To preserve viable cells for transportation or long-term storage, they are typically suspended in a dimethyl sulfoxide (DMSO) solution, frozen slowly, and stored in liquid nitrogen. While this method works well for storing cells on-site, transporting them to other locations can be problematic. Shipping cells in liquid nitrogen is hazardous and very costly. A safer and more affordable alternative is to ship frozen cells using dry ice. Liquid nitrogen boils at -196°C, while dry ice turns directly into gas at -78.5°C. Although cells can be temporarily stored at this temperature, their viability decreases over time, and if the dry ice evaporates or the cells thaw during transport, the viability significantly decreases due to DMSO toxicity [12, 13]. Moreover, new regulations are making it harder to use dry ice for shipping, with more airlines, couriers, and countries imposing stricter controls [12].

Another method involves transporting live cells between laboratories in flasks filled with culture medium. To protect the cells from damage, cells are immersed in culture medium to prevent excessive shaking with air. However, this approach has a major downside: the shipping time is limited to about 24 hours due to the rapid depletion of oxygen and changes in the medium's pH, which can adversely affect the cells. Moreover, transporting liquid samples is problematic in air travel. Thus, developing a more convenient and durable method for shipping live cells would solve many challenges and significantly support scientific research [14].

As traditional methods using dry ice or liquid nitrogen are complex, time-consuming, and can damage cells, the focus has shifted towards alternatives like cell transport containers. The Phoenix™ system is a portable, battery-powered cell transport container designed to keep live-cell cultures safe during long-distance trips. It maintains a stable environment at room temperature, eliminating the need for freezing. The system features an outer container with electronics, power, and heating elements, along with an inner disposable box that maintains a CO_2 atmosphere and sterility [15]. It tracks temperature, humidity, CO_2 levels, and vibrations to ensure optimal conditions during transport. Tests with SH-SY5Y neuroblastoma cells showed that the Phoenix™ system keeps cells just as viable and healthy as standard CO_2 incubators for up to 5 days, even after traveling by ground or air. With over 90% cell viability and normal cell morphology, the Phoenix™ system proves to be a reliable and efficient way to transport live-cell cultures. This innovative technology makes it easier and more cost-effective to transport advanced therapy medicinal products (ATMPs), boosting their accessibility and supporting collaboration and commercialization in cell therapy research and applications. However, the Phoenix™ system has limitations, including a reduced maximum CO_2 measurement of 4% compared to traditional incubators' 5%, and a slight decay in CO_2 levels over five days. Additionally, its battery life limits transport duration, and the system requires capturing a CO_2 atmosphere before sealing, which might not be ideal for longer or more sensitive transports [15].

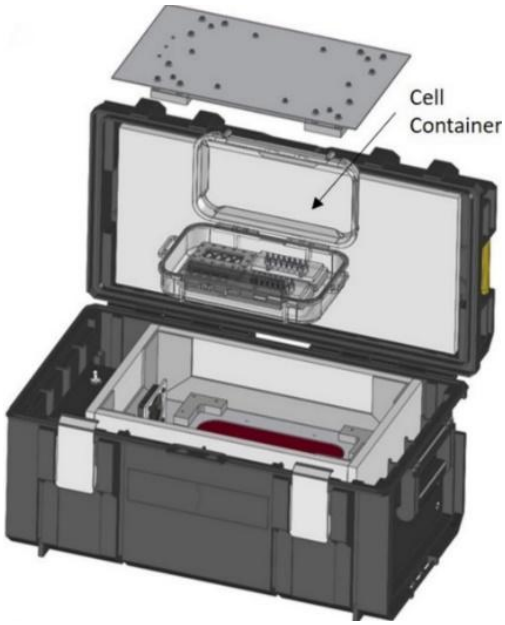

Figure 1. Phoenix system and the internal cell container, which ensures a sterile environment for T-flasks [15].

Another method for cell transportation at room temperature is gel-based techniques. These methods use hydrogels as carriers to keep cells viable and functional during shipping. Hydrogels are three-dimensional polymer networks that hold large amount of water, creating a hydrated environment like natural conditions. Examples of gel-based methods include Agarose-Based Hydrogel, Gelatin-Based Hydrogel, and Alginate-Based Hydrogel [16].

Agarose-Based Hydrogel:

Using agarose gel at an optimal 1% concentration provides the necessary firmness and maintains cell viability during transport. To prepare, dissolve agarose in a medium and mix with cells to form an agarose-based hydrogel. This method preserves cell viability for up to 3 days. Studies have demonstrated that cells retain their appearance and function after transport. It has been successfully tested with MDCK, HEK-293, and A549 cell lines, ensuring high viability and functionality during transportation [14, 16].

Gelatin-Based Hydrogel:

HemSol™ gelatin reagent, a blend of sugars and gelatin, offers a distinct alternative to the dry ice method and has the potential to advance pharmaceutical and biotechnological applications of cells in research. Cells are suspended in the reagent, allowed to gel, and then transported in a sealed, sterile container. HemSol™ gel can protect platelet and red blood cells function in cold storage for up to 6 days, maintaining over 95% cell viability [16].

Alginate-Based Hydrogel:

In this method, cells are encapsulated in alginate hydrogels, creating a biocompatible environment. Sodium alginate is dissolved in sterile water, mixed with cells, and then treated with calcium chloride to induce gel formation. This method is effective for transporting stem cells and other sensitive cell types in regenerative medicine and tissue engineering, demonstrating high survival rates of 74% for mouse embryonic stem cells and 80% for human mesenchymal stem cells after 5 days at ambient temperatures. The stability of alginate gels can be further enhanced with cross-linking agents like strontium [16, 17].

Another innovative approach for transporting live cells at ambient temperature is to use Transwell inserts. Transwell inserts are essential for transporting intact cell and tissue constructs between facilities while maintaining their viability and functionality. These inserts fit into multi-well plates and support both anchorage-dependent and anchorage-independent cell lines. A specially designed transport device for Transwell inserts ensures cell viability during shipping by providing a stable environment at room temperature, avoiding the need for hypothermic preservation. This device includes a Transwell carrier and a sealing lid, filled with medium to keep cells hydrated and protected. Tests with cell lines such as Caco2, A549, and HepG2 C3A showed high viability rates above 97% after 48 hours of simulated shipping. Additionally, complex constructs like blood-brain barrier models showed that their integrity could recover after shipping, demonstrating the effectiveness of the device. This innovation facilitates safe transfer and collaboration between labs [11].

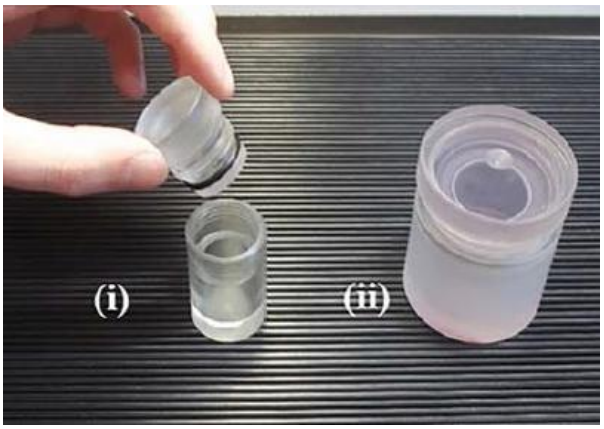

Figure 2. Transwell transporting device for the insert of a 24-well plate (i) and a 6-well plate (ii) [11]

1.1 Cryopreservation

Research on low-temperature tissue storage began in the late 1800s, leading to significant advancements in cryopreservation techniques [18]. Cryopreservation is a method used to maintain the structural integrity of living cells and tissues by cooling them to very low temperatures for extended periods. This process slows down biological and chemical reactions within cells, making long-term storage possible. However, freezing causes significant challenges due to the formation of ice crystals inside and outside cells, which can lead to mechanical stress and cellular damage. A major challenge in cryopreservation is controlling the transition of water to ice [19]. Rapid cooling typically causes intracellular ice formation, while slow cooling can induce osmotic stress due to highly concentrated solutes and mechanical interactions with extracellular ice [19, 20]. Cryoinjury, the damage resulting from phase changes in water at low temperatures, is primarily attributed to osmotic rupture from concentrated solutes and intracellular ice formation, both of which are influenced by the cooling rate [19].

To address these issues, cryoprotective agents (CPAs) are used. CPAs play a crucial role in modifying the freezing behavior of cells by controlling water transport, nucleation, and ice crystal growth, thereby protecting cells from damage during freezing. The response to cryopreservation can vary widely among different cell types and mammalian species [19, 21].

The main approaches to cryopreservation include slow freezing, which involves gradual cooling to prevent the formation of intracellular ice; vitrification, which rapidly cools cells to transform their aqueous environment into a glass-like state, thus avoiding ice formation; and subzero nonfreezing storage, where cells are maintained at subzero temperatures without actual freezing. Critical steps in cryopreservation include mixing cells or tissues with CPAs before cooling, cooling and storing the samples at low temperatures, warming the samples, and finally, removing the CPAs after thawing. The careful application of CPAs is essential to ensure the viability of the preserved samples [19].

Traditional CPAs, such as dimethyl sulfoxide (DMSO), have been widely used due to their efficacy. However, DMSO is known for its cytotoxicity, particularly at ambient temperatures, which necessitates the search for less harmful alternatives [16].

Recent advancements in cryoprotective agents signify a major shift towards safer and more effective cell preservation techniques [22]. The development of non-toxic alternatives to DMSO, such as glycerol, proline, ectoine, and betaine, along with innovative methods like bio-inspired cryo-ink, which forms protective nanoliter droplets using ectoine, trehalose, and polyethylene glycol, and trehalose-based formulations, that stabilize cell membranes and proteins through hydrogen bonding, presents promising solutions for maintaining cell viability during cryopreservation [16].

Currently, there are commercially available cryosolutions, including DMSO-based options with lower concentrations of DMSO like NutriFreez® D10 and CryoStore®CS10, as well as DMSO-free alternatives such as Pentaisomaltose™, CryoScarless™, CryoNovo P24™, StemCell Keep™, CryoSOfree™, and XTThrive™. However, the quality and effectiveness of these solutions in protecting a wide range of cellular therapeutics have not been thoroughly investigated. Further research is necessary to evaluate the compatibility of these cryoprotectants with various biotherapeutics [23, 24].

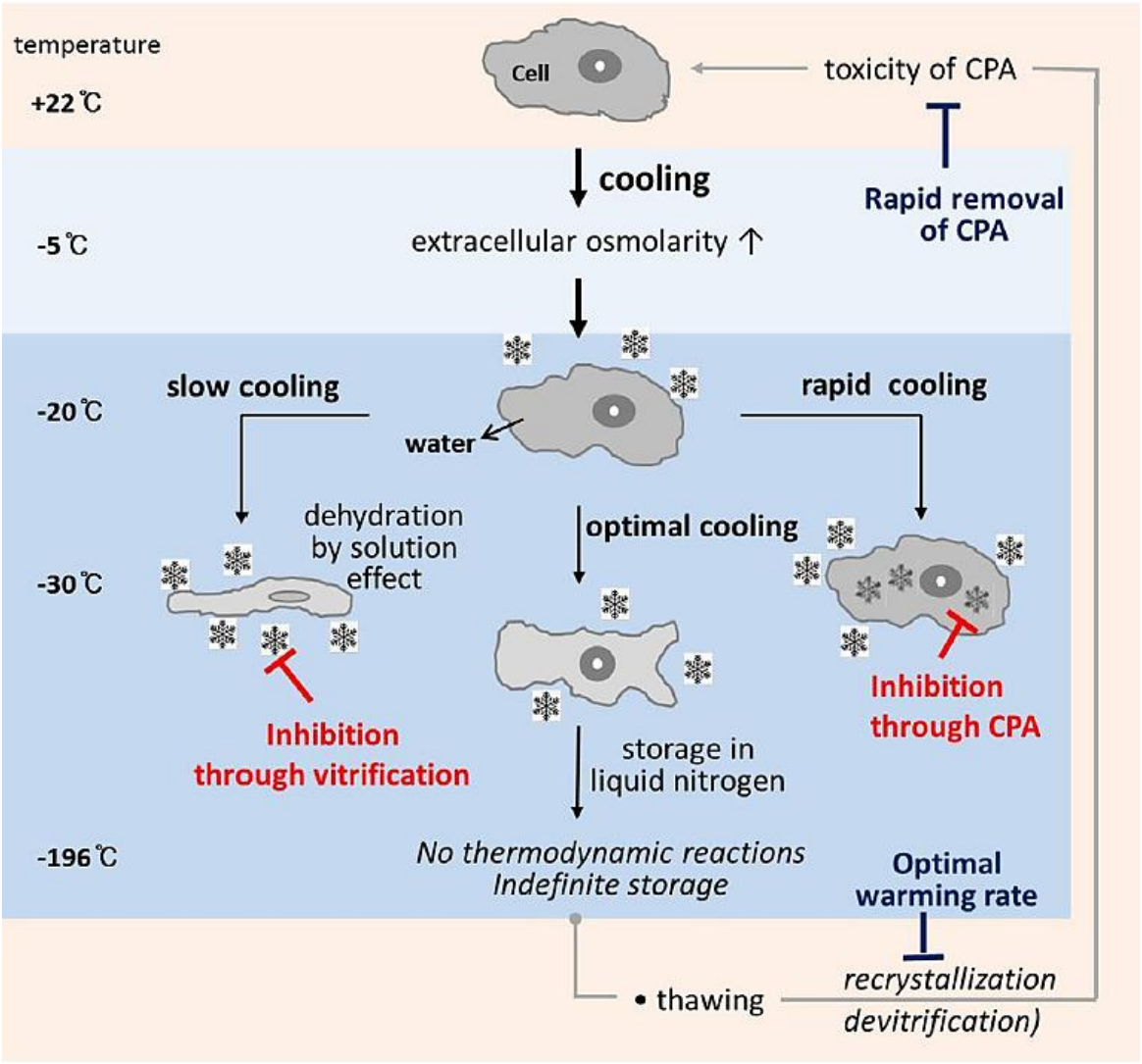

Figure 3. Cryoinjury processes of cells during freezing and thawing [19]

1.2 Multicellular Spheroids

Cell culture is a common *in vitro* method utilized to enhance our comprehension of cell biology, tissue structure, disease mechanisms, drug effects, protein synthesis, and tissue engineering development [25].

For more than a hundred years, researchers have relied on two-dimensional (2D) cell cultures as *in vitro* models to examine cellular reactions to biophysical and biochemical cues. Although these techniques are well-established and have substantially advanced our understanding of cell behavior, emerging evidence indicates that 2D systems may sometimes produce cellular activities that deviate significantly from those seen *in vivo*. For instance, certain properties of cancer cells are not completely represented in 2D cultures [26, 27].

Cells in the human body interact with neighboring cells and the extracellular matrix (ECM) to form a complex three-dimensional structure essential for normal function. In two-dimensional monolayer cultures, cells often lose their tissue-specific properties. In recent decades, researchers have focused on creating three-dimensional (3D) cell culture models to connect cell-based assays and animal studies, reducing uncertainties and costs, for example for drug screening purposes [28].

3D culture systems provide an exceptional method for growing cells (such as cancer cells) either alone or alongside various other cell types in a spatially relevant manner. This approach promotes cell-cell and cell-matrix interactions, which can closely replicate the natural tumor environment. Consequently, cells cultured in 3D acquire morphological and cellular characteristics that are representative of *in vivo* tumors. For instance, breast cancer cells co-cultured with luminal cells, myoepithelial cells, and stromal fibroblasts in a 3D setup exhibit features similar to those of ductal carcinoma *in situ* [29].

In scientific literature, the terms "organoids," "spheroids," and "3D cell cultures" are frequently used interchangeably. Spheroids are spherical cell clusters cultured as free-floating aggregates and are generally considered to have a simpler structure that less accurately replicates tumor architecture [30, 31].

Conversely, organoids are 3D-grown cells that form structural units resembling an organ's architecture and function to a significant degree. 3D cultures can be established using ECM support (scaffold-based) or without a scaffold (scaffold-free). While both spheroids and organoids serve distinct and overlapping purposes, they differ in their sources of tumor cells, culture protocols, and the time required for their establishment [30, 31]. Following figure demonstrate a comparison of the main characteristics of monolayer cell cultures, spheroids, and organoids [32].

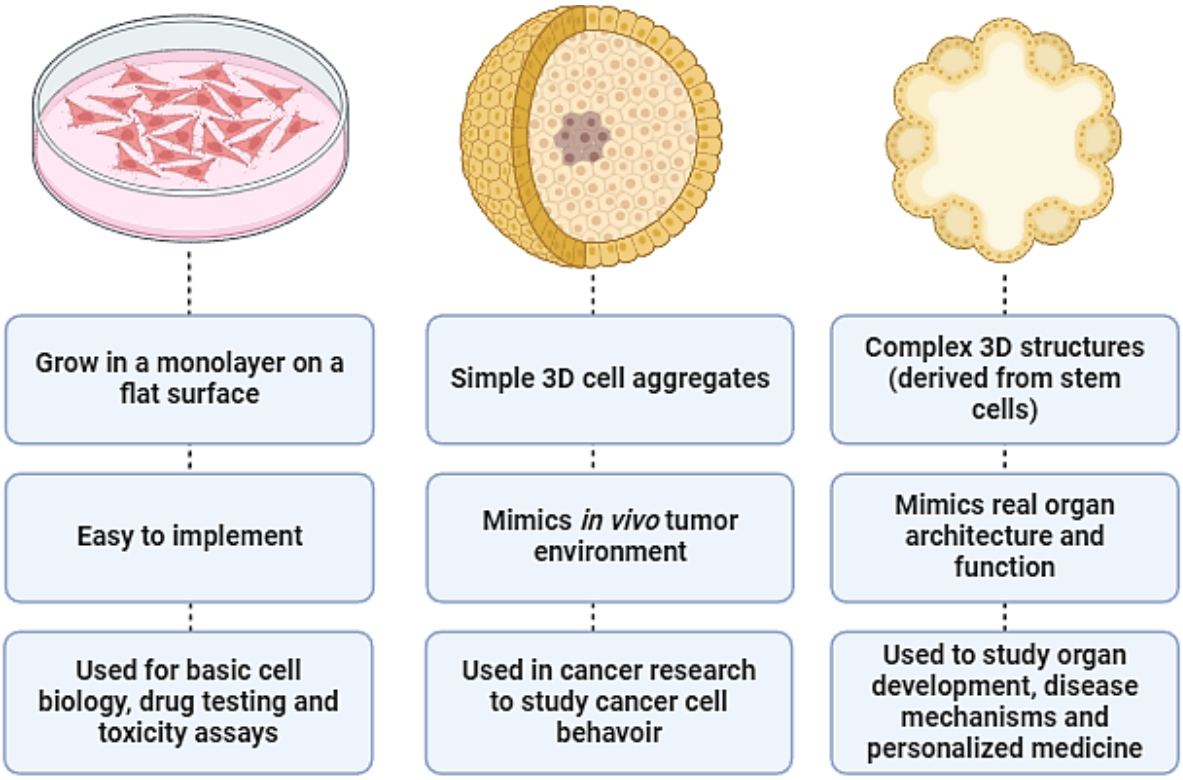

Figure 4. A comparison of the main characteristics of monolayer cell cultures, spheroids, and organoids. created with BioRender.com

1.3 Spheroid Formation

Spheroid formation is one of the most well-characterized models for 3D cell culture, as they closely mimic the architecture and function of physiological tissues [33, 34]. The formation of spheroids involves several stages, fundamentally regulated by molecules such as cadherin and integrin. These molecules play a key role in the mechanisms that drive spheroid assembly and stability [35]. Initially, individual cells in suspension come together to form loosely bound spheroid clusters. At this stage, interactions between extracellular matrix fibers and integrins on the cell surface facilitate early aggregation. Subsequently, E-cadherin enhances the adhesion among the initial cell clusters through homophilic binding with cadherins on adjacent cells. Moreover, the β-catenin complex plays a pivotal role in mediating cellular signal transduction. Additionally, actin contributes to the clustering and maintenance of cellular 'stemness' by reinforcing contacts among neighboring cells. This coordinated series of interactions and processes ultimately leads to the formation of robustly adhesive spheroids [30, 36].

E-cadherin (CDH1), a calcium-dependent homophilic transmembrane adhesion molecule, is recognized as a crucial factor in spheroid formation. Its effects have been substantiated through studies involving human breast cancer cell lines and mouse embryonic stem cells. Research on mouse embryonic stem cells demonstrated that E-cadherin-mediated cell adhesion is crucial for embryonic body aggregation. Blocking E-cadherin activity with antibodies significantly hinders this process. Integrins, composed of α- and β-subunit heterodimers, are essential for cell-ECM interactions during cell invasion and migration. Both E-cadherin and β1-integrin are important in the early stages of spheroid formation, with integrin-ECM interactions significantly influencing the rate of multicellular spheroid formation [35-37].

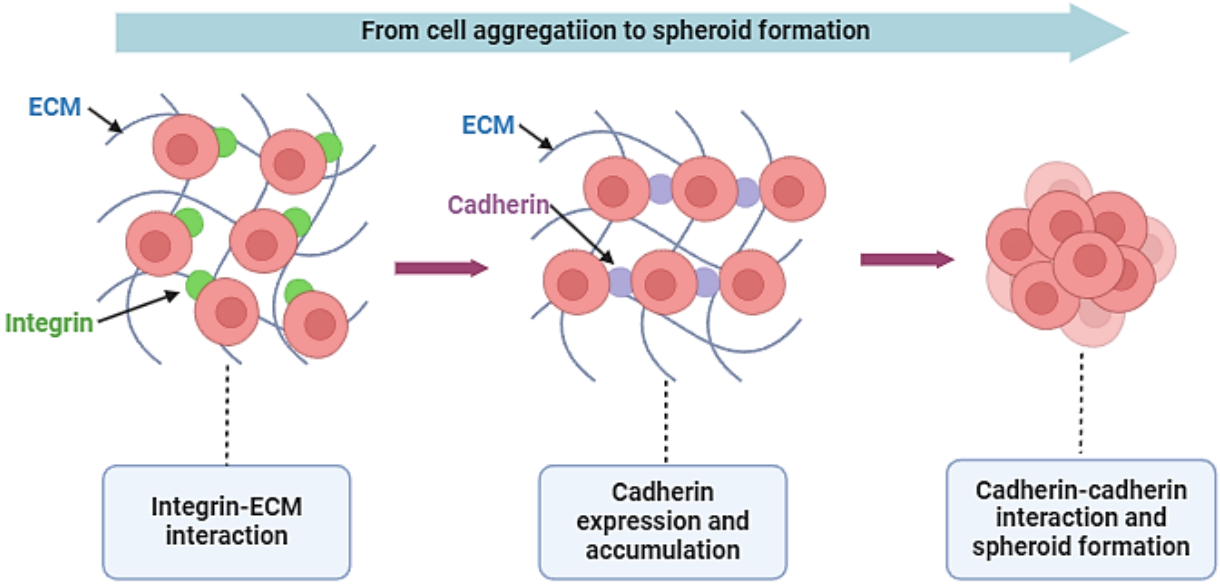

Figure 5. Spheroid formation involves ECM-integrin aggregation, cadherin-driven compaction, and dense cadherin interactions. created with BioRender.com

Spheroids typically exhibit gradients in oxygen levels, nutrient distribution, metabolic waste accumulation, and proliferation profiles. Spheroids with diameters exceeding 400–500 µm often develop a concentrically layered structure: a necrotic core, surrounded by a viable layer of quiescent cells, and an outer rim of proliferating cells. The peripheral cells closely mimic the *in vivo* environment of actively proliferating tumor cells adjacent to capillaries, while the inner cells remain quiescent or die through necrosis and apoptosis. Numerous studies have characterized the oxygen profiles within various types of spheroids, revealing characteristic oxygen tension patterns [38].

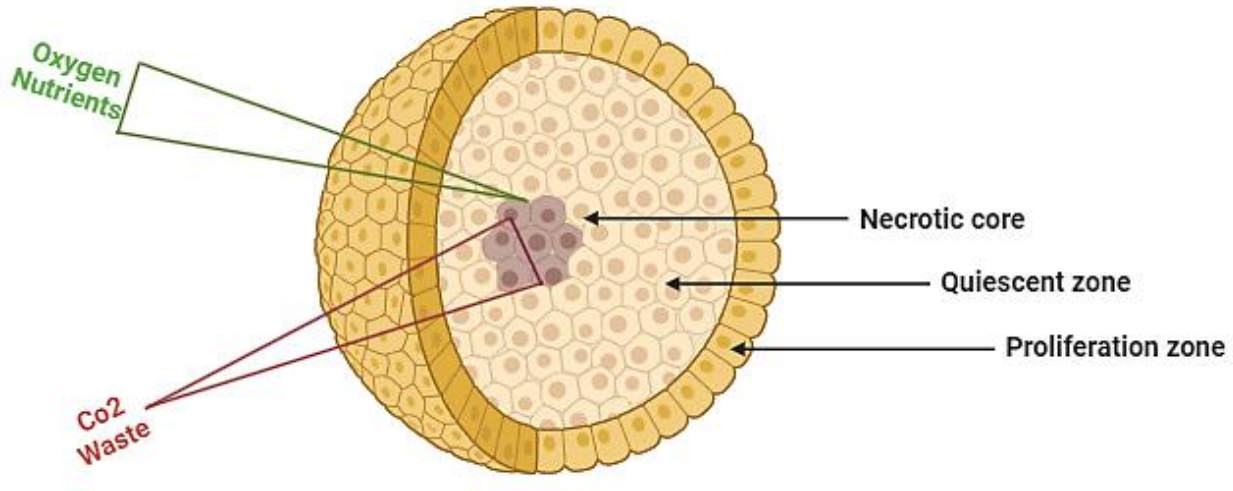

Figure 6. Spheroids naturally form gradients of nutrients, oxygen, leading to a central necrotic core, a surrounding layer of quiescent viable cells and outer layer of proliferating cells. created with BioRender.com

1.4 Conventional Methods of Spheroid Formation

1.4.1 Pellet Culture:

The pellet culture technique uses centrifugal force to concentrate cells at the bottom of a conical tube, promoting cell-to-cell adhesion. Typically, a cell suspension is first pre-incubated on a shaker to enhance spheroid formation and then centrifuged. This method is favored for its simplicity and rapid creation of spheroids, making it commonly used in studies of chondrogenesis, bone formation, and mesenchymal stem cell differentiation. Pellet culture has drawbacks, including potential cell damage from shear stress during centrifugation and hypoxia in large spheroids, which can cause necrosis in some cells while promoting chondrocyte differentiation. The technique is also not scalable for mass production, and cell aggregation cannot be visualized during the process [39, 40].

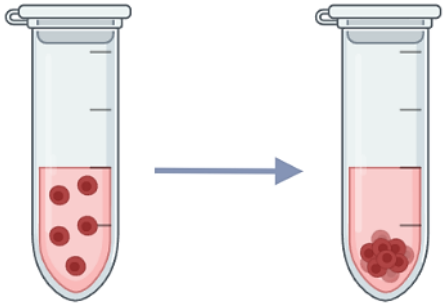

Figure 7.Pellet culture, created with BioRender.com

1.4.2 Liquid Overlay:

The liquid overlay technique, also known as static suspension culture, creates spheroids by preventing cell adhesion on non-adherent culture plates. This technique typically uses a layer of agar or agarose gel, with agarose being particularly effective due to its excellent non-adherent properties. As cells cannot attach to the surface, they spontaneously aggregate and form spheroids, facilitated by cell-cell adhesion molecules [35, 41].

Although agarose offers several advantages, it presents limitations in culturing cancer cells due to its lack of interaction with cancer cell receptors. In substitution, hyaluronic acid (HA) represents a promising alternative to agarose gel for cancer cell culture, as it is more suitable for spheroid assembly and facilitates HA-cell surface receptor interactions [42, 43].

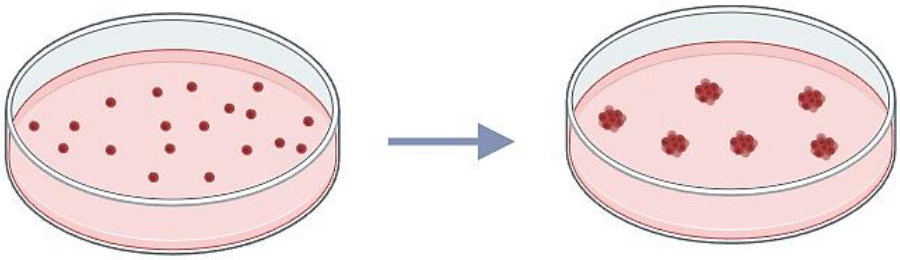

Figure 8.Liquid overlay method, created with BioRender.com

1.4.3 Hanging Drop:

In 1995, Keller introduced the hanging drop method to investigate the differentiation of embryonic stem cells *in vitro*. This technique utilizes gravity to concentrate cells at the bottom of hanging droplets, forming spheroids over time. A small drop of cell suspension, usually less than 50 µL, is placed on the lid of a microplate, which is then inverted, allowing the cells to settle at the bottom of the droplet due to gravitational force. This method, when used with microplates, enables high-throughput preparation of cell spheroids [44]. The hanging drop system provides several benefits beyond the ability to control spheroid size. It is cost-effective and does not require expensive or specialized equipment for small-scale experiments [30, 35]. Large quantities of spheroids can be efficiently produced using multichannel pipettes, and they can be easily harvested by scraping the lids of culture dishes. Additionally, mesenchymal stem cells cultured using this method can produce substantial amounts of powerful anti-inflammatory and anti-tumorigenic factors [30, 35].

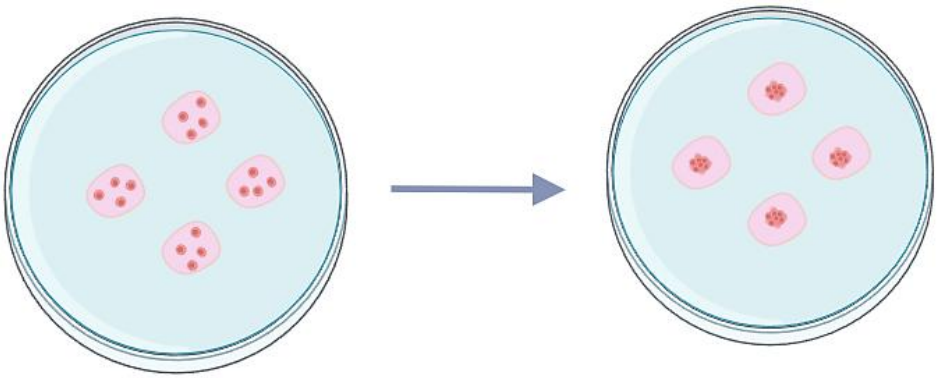

Figure 9. Hanging drop method, created with BioRender.com

1.4.4 Spinner Culture (Spinner Flask):

The spinner flask is a traditional tool for developing dynamic culture bioprocesses at the laboratory scale. This system features a cylindrical glass or plastic flask equipped with an impeller to facilitate mixing, ideally at low shear stress. Common impeller designs include paddle and bulb shapes. Spinner flasks effectively produce spheroids from various tumor cell lines, with diameters ranging from 80 to 300 µm, depending on the cell line, mixing rate, and culture duration. Some cell lines form uniform spheroids, while others create irregular structures due to varying culture conditions [45, 46].

However, higher shear stress can cause cell damage and physiological changes. Non-uniform shear stress and diverse conditions complicate data comparison and hinder the development of consistent culture protocols [45, 46].

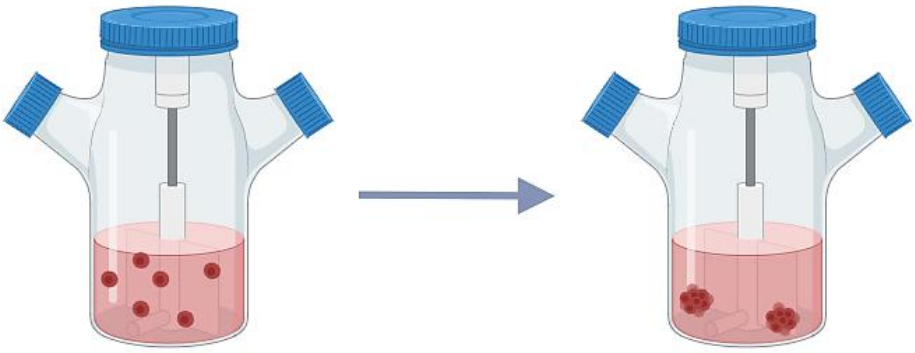

Figure 10. Spinner flask, created with BioRender.com

1.4.5 Rotating Wall Vessel (RWV):

Developed by NASA in 1992, rotating wall vessel (RWV) bioreactors are designed to study cell growth under simulated microgravity conditions. These bioreactors operate by rotating the culture chamber along a horizontal axis, keeping cells in constant suspension and preventing them from adhering to the chamber walls [47, 48]. By adjusting the rotation speed, low shear forces are maintained, promoting optimal cell-cell interactions and the formation of larger 3D structures. Continuous rotation also prevents spheroid coalescence, leading to uniformly sized spheroids. This method is well-suited for long-term 3D spheroid culture, as it allows for easy medium replacement, facilitating efficient nutrient supply and waste removal. The main limitation is the requirement for specialized equipment [47].

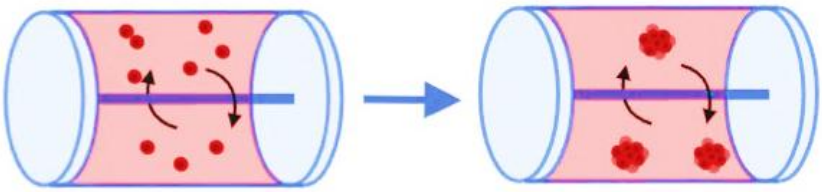

Figure 11. Rotating wall vessel, created with BioRender.com

1.4.6 Magnetic levitation:

Magnetic levitation is another technique used for creating 3D cell cultures by levitating cells using magnetic forces, allowing them to maintain cellular activity and producing ECM [49, 50]. In the magnetic levitation method, cells treated with paramagnetic nanoparticles are seeded into low-adhesive plates and pulled upwards by a magnet to form spheroids. Alternative approaches use gadolinium (III) chelates or hydrogels with nanoparticles to enhance 3D culture formation and viability [49]. This method is valuable for studying cancer cells and cellular interactions, providing a cost-effective alternative to expensive xenograft models. However, it requires careful handling of paramagnetic agents and nanoparticles. The uniformity and reproducibility of the cultures can vary, necessitating further validation against established models [49].

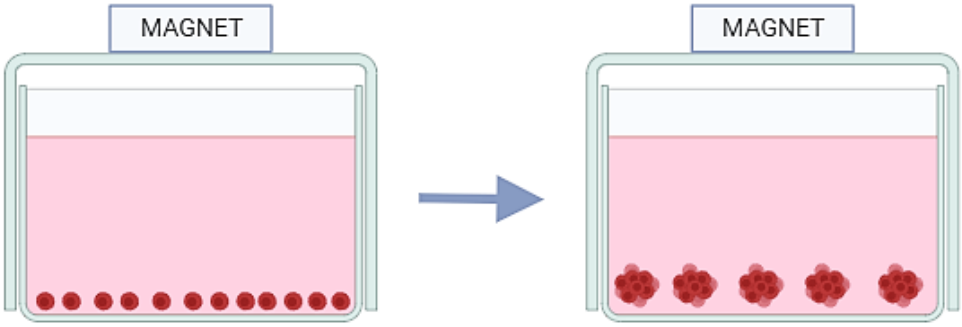

Figure 12. Magnetic levitation, created with BioRender.com

1.5 Microfluidic Technology, an Innovative Method for Spheroid Formation

Microfluidics involves the study of fluid flow within micro-scale geometries, offering unique properties that enable cost-effective reagent handling. The field began to gain attention with Stephen Clark Terry's demonstration of a microfabricated silicon gas chromatographic analyzer in 1975. By reducing volumes, this technology lowers the cost of expensive reagents and increases the relative surface area, resulting in faster reaction times. Microfluidic systems typically operate within volume scales of 100 nanoliters to 100 microliters and feature sizes ranging from 1 to 1000 micrometers [51, 52].

At these scales, forces like surface tension and capillary action dominate over gravity. This allows for tasks such as passive fluid pumping, precise surface patterning, analyte filtration, and creating uniform droplets in fluid streams [53].

Microfluidic technology significantly advanced in 1990 when Manz et al. proposed the concept of integrating multiple laboratory functions on a single microchip, leading to the development of lab-on-a-chip (LOC) systems [52]. Lab-on-a-chip (LOC) technology has emerged as a pivotal innovation in microengineering, encapsulating the miniaturization and integration of complex laboratory processes into a single microchip. This technology addresses several critical practical challenges by offering a compact, efficient, and cost-effective solution for performing chemical, biological, and biochemical analyses [54, 55].

LOC systems significantly reduce reagent consumption and integrate multiple laboratory functions into a cohesive platform, facilitating high-throughput and high-precision experimentation. The development of LOC devices involves the intricate design of microfluidic channels and components, which control the flow and interaction of minute fluid volumes with remarkable accuracy [54].

Advances in microfluidics have revolutionized diagnostics with precise, rapid, and affordable tests, aiding therapeutic development through antibody screening and drug testing. They also boost food safety by detecting pathogens and control reactive streams for continuous production of materials, including pharmaceuticals, with applications in personal care and drug delivery [56].

1.6 Organ on a chip (OoC)

After the advances in microfluidic devices in the late 1990s, microfluidic systems have been developed to mimic organ functions, leading to the creation of liver, lung, intestine, and kidney-on-a-chip models [57]. An organ-on-a-chip is a cell culture model featuring microfluidic channels, designed to replicate the activities and physiological responses of a whole organ [58]. This method integrates 3D ECM, biochemical factors, and biophysical cues. Recent advancements in microfluidics-based OoC technology, or microphysiological systems, could transform drug development and personalized medicine by replacing animal testing [59, 60].

Even with their simplicity, OoC systems effectively mimic human physiological and pathological conditions. These advanced *in vitro* models recreate the *in vivo* environment, enabling biological experiments outside the body [61]. Furthermore, OoC systems enable detailed, cost-effective, and high-throughput drug studies and disease modeling [62]. The effectiveness of an organ-on-a-chip (OOC) *in vitro* model depends on the harmonious integration of device engineering, cell biology, and biomarker discovery [63].

1.7 Spheroid on a Chip

For developing *in vitro* multicellular spheroids and organoids, creating and refining the microenvironment is essential. Traditional culture methods depend on random self-assembly or self-organization, which lack the chemical gradients and mechanical forces typical of *in vivo* microenvironments. Therefore, engineering strategies are required to improve the cultivation success of spheroids and organoids *in vitro*. Advancements in micro-nano fabrication have made microfluidic technology essential for overcoming challenges in conventional spheroid and organoid cultures. These devices precisely control fluid volumes at a microscale, matching the size of spheroids and organoids, which leads to low sample consumption and improved observation and analysis [64-66].

Microfluidic technology significantly advances the development of spheroids and organoids by providing several key enhancements. Firstly, it offers spatial-temporal control, adjusting biochemical signals and structural arrangements to closely mimic *in vivo* environments. Secondly, it models mechanical cues by replicating natural physical forces such as shear stress and compression that cells encounter. Thirdly, it enables high-throughput analysis, allowing for the simultaneous processing and examination of numerous samples, thereby enhancing experimental efficiency. Additionally, microfluidics facilitates the interaction of multiple tissues or organoids on a single platform, promoting complex biological interactions. Finally, it integrates biosensing and bioimaging technologies, incorporating sensors and imaging techniques to continuously monitor and visualize cellular activities, thus providing a comprehensive analysis of cellular behavior and function [64, 65].

Recent microfluidic advancements enable precise control of spheroid size and growth but still lack automated 3D spheroid generation and multi-size production on a single platform, essential for studying size-dependent drug responses and toxicities. To address the rising need for medium-throughput and high-content multicellular spheroid systems, future microfluidic devices should ensure optimal tissue culture environments with accurate control over medium composition and gas exchange, facilitate easy and reliable cell loading processes, enable simultaneous production of spheroids in multiple sizes, incorporate dynamic medium perfusion capabilities and offer user-friendly operation and consistent tissue maintenance [67].

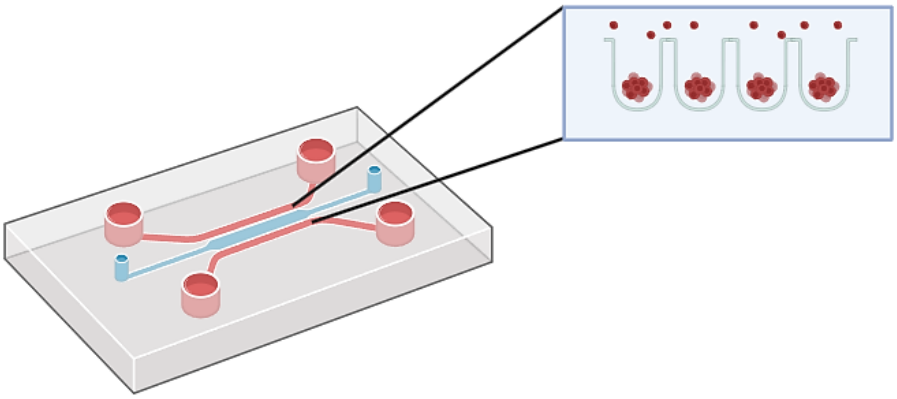

Figure 13. Spheroid on a chip, created with BioRender.com

1.8 Methods in Microfluidic Device Fabrication

The field of microfluidics now offers a broad array of materials and methods, increasingly accessible through heightened research efforts. This diversity enhances the potential for technological advancements and adoption, facilitating new opportunities for development in both academia and industry [68].

Initially, microfluidic devices utilized silicon and glass, but the introduction of polymers in the late 1990s shifted the focus due to their cost-effectiveness and diverse properties. Polymer fabrication is straightforward, requiring no hazardous chemicals and cheaper equipment, making it accessible for research labs and driving both academic and industrial development [69, 70].

Polymer materials used in microfluidic applications fall into two main categories: polydimethylsiloxane (PDMS) and thermoplastics. Thermoplastics, include poly(methyl methacrylate) (PMMA), polycarbonate (PC), polystyrene (PS), polyvinyl chloride (PVC), polyimide (PI), and cyclic olefin polymers like cyclic olefin copolymer (COC), cyclic olefin polymer (COP), and cyclic block copolymer (CBC) [69-72].

PDMS is favored in microfluidic applications for its high gas permeability, excellent optical clarity, and biocompatibility, which are beneficial for complex designs and high-throughput applications. However, it can swell in certain solvents and has lower mechanical stability, leading to sample absorption and leaching issues. In contrast, thermoplastics offer high mechanical stability, low water absorption, and resistance to solvents and acids, making them cost-effective and suitable for chemically durable applications, though they are less flexible than PDMS [69].

Microfluidic structure fabrication depends on the compatibility of materials and methods. Traditional approaches, including deposition, lithography, and etching, were primarily used for glass and silicon, focusing on 2D channel production through plasma or chemical etching. These techniques, while effective, are often expensive, time-intensive and require precise parameters. Modern methods, designed for polymers, encompass soft lithography, injection molding, laser micromachining, and bonding. These microfluidic fabrication methods often do not achieve true three-dimensional architecture or design flexibility, making modifications challenging. These techniques also typically require a cleanroom environment to ensure accuracy [73-75].

A more effective fabrication approach is essential for cheaper, easier, and faster prototyping of microfluidic devices in a range of materials. Recently, 3D printing has emerged as a practical alternative, offering several advantages. It allows for easy design edits and reprints, facilitating optimization without the need for a cleanroom. The consumables are mainly resin and solvent, keeping costs low. Additionally, 3D printing can achieve fully three-dimensional structures, enabling unique device capabilities [75].

This technique is a layer-by-layer manufacturing method that constructs intricate objects directly from digital files. It starts by importing 3D models from Computer-Aided Design (CAD) programs or 3D scanners. Next, slicer software generates a series of layers along the Z-axis from these models. Finally, the object is created by sequentially printing and stacking each layer [76].

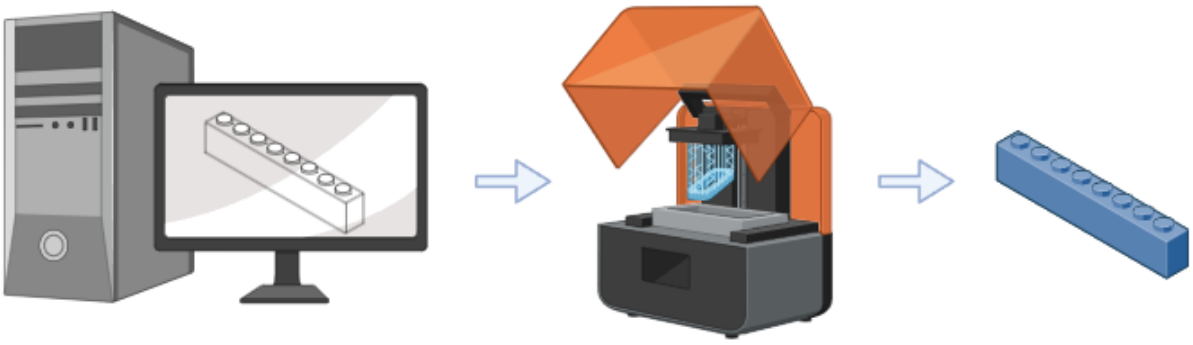

Figure 14. 3D printing process, including preprint phase (computer design), layer by layer printing and post printing phase, created with BioRender.com

1.9 Aim

The main objective of this thesis is to develop, validate, and optimize a novel method for transporting mammalian living cells using the Cryosphere device, which is designed for the preservation, transportation, and recultivation of spheroids. The Cryosphere device will be engineered to facilitate spheroid formation, ensure structural integrity during preservation and transportation, and be user-friendly for practical applications. This study aims to address the limitations of existing cryopreservation techniques and provide a robust solution for maintaining spheroid viability and functionality from formation to end-user application.

A key component of this thesis is to identify the most effective cryoprotectant solutions suitable for both preservation and room temperature incubation, which is critical for transportation. This involves rigorous testing of various combinations of cell culture media and cryoprotectants to determine the best conditions for maintaining spheroid viability and morphology.

The study also aims to demonstrate the versatility and effectiveness of the Cryosphere device with the proposed workflow, as illustrated in Figure 15, which involves seeding a cryotube with a cell suspension, allowing spheroid formation over a three-day period, and then freezing the sample. When required, the sample can be thawed and shipped at room temperature without media exchange. After thawing and shipment, the spheroids are processed through digestion, and the resulting cells are prepared for re-cultivation. This workflow, in combination with the Cryoinsert device, addresses key challenges in live-cell shipment by reducing labor intensity and costs, while ensuring consistent cell viability and functionality. These improvements have significant potential to advance applications in cell banking, cell shipping, and regenerative medicine.

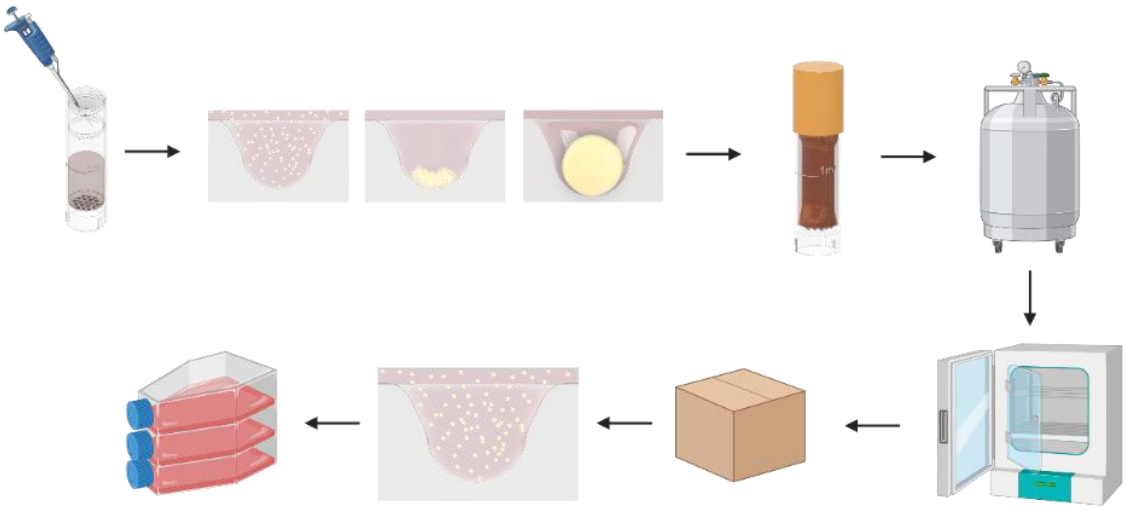

Figure 15: Workflow of spheroid formation, freezing, thawing, and shipping using the Cryosphere device, created with BioRender.com

2. Material and Methods

2.1 Cell culture

The initial phase of the study focused on cultivating 2D and 3D cell cultures, using 2 cell lines, HEK (Human Embryonic Kidney 293) and HeLa (Henrietta Lacks' cell) cells. Both cell lines provided by Medical University of Graz.

To ensure sterility, all procedures were carefully carried out under a laminar flow hood, with all surfaces and materials disinfected using 70% ethanol.

2.1.1 Normal Growth Media (NGM)

For HEK 293 cells, the normal growth medium used was DMEM-F12 (Sigma Aldrich), while HeLa cells, were maintained in DMEM high glucose medium (Sigma Aldrich). Both mediums were supplemented with 10% fetal bovine serum (FBS, Sigma Aldrich) and 1% antibiotic/antimycotic solution (AB, Sigma Aldrich).

2.2 2D Cell Cultivation Process

First, frozen cell vials were retrieved from a nitrogen tank at -196°C and rapidly thawed in a 37°C water bath (VWR). Warm NGM was slowly added to the cell suspension, which was then transferred to a falcon tube (Greiner Bio-One). The cell suspension was centrifuged at 1200 rpm for 5 minutes to pellet the cells. The supernatant was carefully discarded. The pellet was resuspended in fresh NGM, and the resuspended cells were transferred to cell culture flasks (Greiner Bio-One). containing fresh NGM. For T25 flasks, approximately 0.7 x 10^6 cells were seeded with 3-5 ml of NGM; for T75 flasks, 2.1 x 10^6 cells were used with 8-15 ml of NGM; and for T175 flasks, 4.6 x 10^6 cells were seeded with 15-30 ml of NGM. The flasks were incubated under standard conditions (37°C and 5% CO_2) for further experiments.

For seeding, the adherent cells were discarded from the flask once they reached 90% confluency. The process began with removing the old media from the flask, followed by washing the flask with phosphate-buffered saline (PBS, Sigma Aldrich).

Trypsin-EDTA (Gibco) was then used to detach the cells from the surface, with 1 ml for T25 flasks, 2 ml for T75 flasks, and 5 ml for T175 flasks. The flasks were incubated at 37°C for 3-5 minutes, then gently tapped to facilitate cell detachment, The trypsinized cells were rapidly neutralized with warm NGM at twice the volume of Trypsin-EDTA used. The cell suspension was transferred to a Falcon tube for centrifugation. After centrifugation, the resulting cell pellet was resuspended in the desired amount of NGM. For cell counting, 10 µl of the cell suspension was mixed with 10 µl of trypan blue (Sigma Aldrich) and the mixture was transferred to a Neubauer cell counting chamber. The concentration of viable cells per mL was determined by dividing the number of live cells counted by the number of large corner squares counted, then multiplying by both the dilution factor and 10,000.

Similarly, the concentration of non-viable cells was calculated using the count of dead cells. The percentage of cell viability was calculated by dividing the number of viable cells by the total number of cells and multiplying by 100. To maintain actively growing cultures, cells were split once a week when they reached approximately 90% confluency.

Additionally, the media of the flask was replaced with fresh NGM once a week to provide essential nutrients and remove waste. For splitting, the cells were detached using Trypsin-EDTA as described above. They were then centrifuged to form a pellet, which was subsequently resuspended in the desired amount of fresh NGM. For example, HEK cells required splitting once a week at a ratio of 1:4, meaning one-fourth of the cell suspension was transferred to a new T75 flask containing fresh NGM. Specifically, HeLa cells were split at a ratio of 1:6 per week.

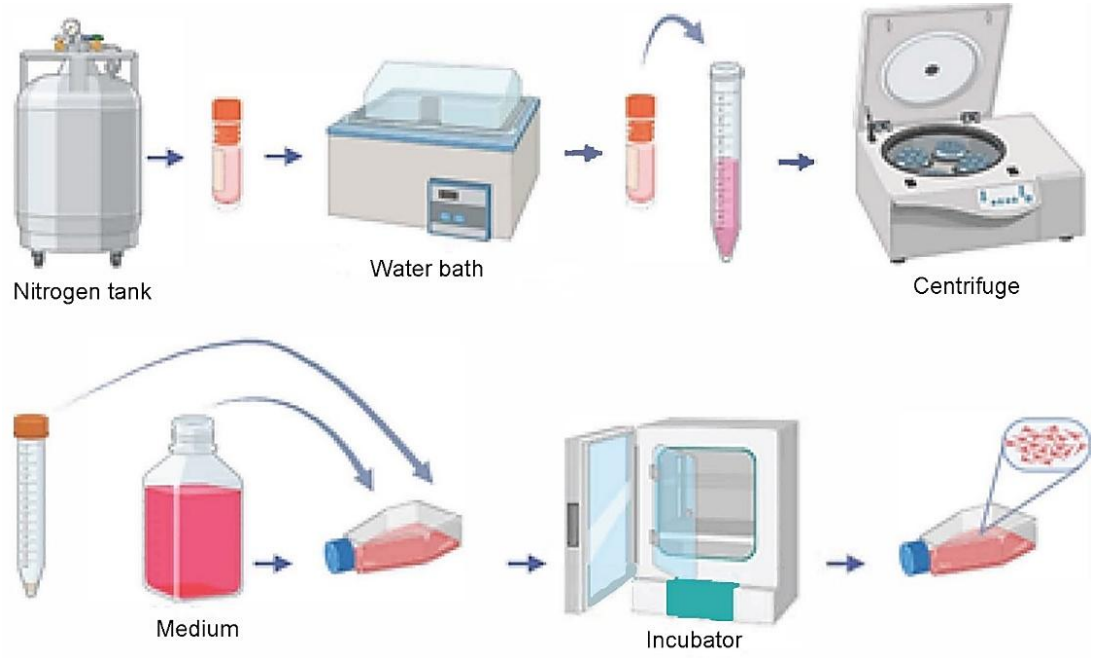

Figure 16. 2D cell cultivation process, created with BioRender.com

2.3 3D Cell Cultivation Process

The process of cultivating 3D cell cultures begins with the preparation of a U-bottom 96 well plate. Each well is coated with 100 µL of FLEX coating solution (faCellitate) to prevent cell adhesion and support spheroid formation. The plate was incubated at room temperature for 3 minutes, after which the excess coating solution was carefully discarded by gentle aspiration. It was then incubated for an additional 30 minutes at room temperature. Following this, a cell suspension was prepared, and the cells were accurately counted.

Subsequently, 7,500 cells are seeded into each well of the U-bottom 96 well plate (Corning), followed by the addition of 200 µL of NGM. To facilitate spheroid formation, the U-bottom 96 well plate is centrifuged at 1000 rpm for 5 minutes. After centrifugation, the plate is incubated at 37°C with 5% CO_2, allowing spheroid formation within 3 days. During this period, the cells are monitored daily using a microscope (Olympus).

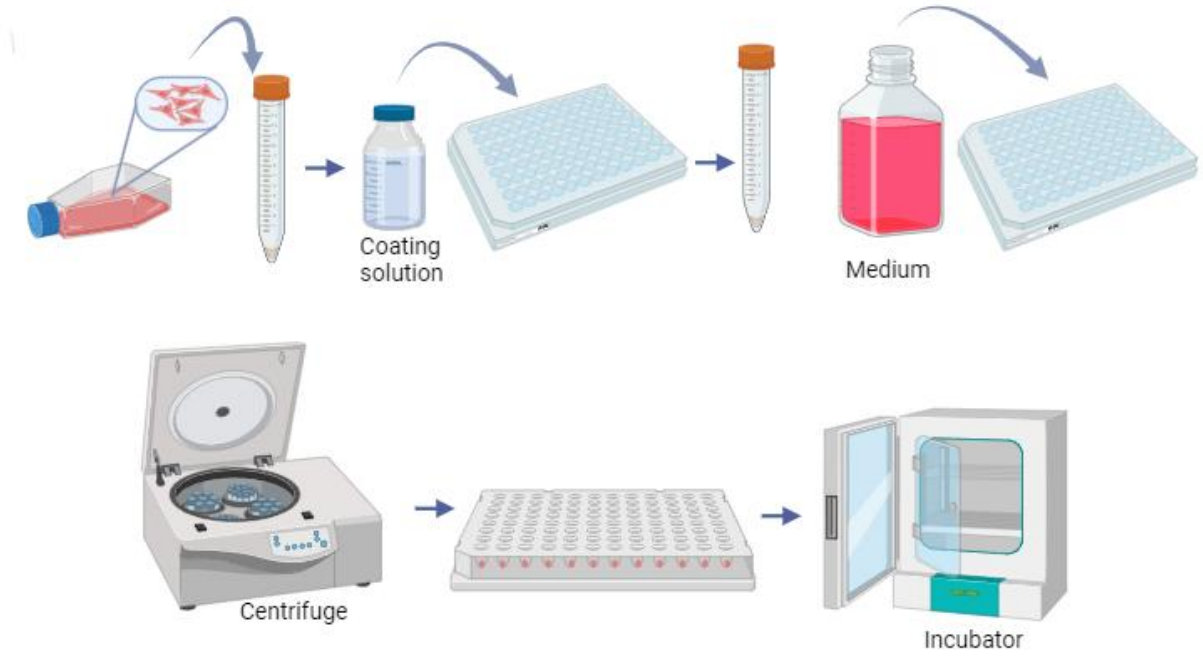

Figure 17 .3D cell cultivation process, created with BioRender.com

2.4 Media Selection Procedure for Optimal Cell Viability at Room Temperature Cultivation

Various combinations of cell culture mediums and cryoprotectants were evaluated to determine their effects on cell viability during room temperature cultivation.

2.4.1 Culture Mediums & Cryoprotectants

The cell culture mediums used included Normal Growth Media and CO_2 independent buffer systems such as CO_2 independent medium (Thermo Fisher Scientific), Hibernate A medium (Thermo Fisher Scientific) and Hibernate E medium (Thermo Fisher Scientific). All the mediums were supplemented with 10% FBS and 1% AB.

Commercial cryoprotectants utilized were DMSO (dimethyl sulfoxide, Chem Cruz), Nutrifreez D10 cryopreservation medium (Nutrifreez, Sartorius), and CryoSOfree DMSO-free cryopreservation medium (CryoSOfree, Sigma Aldrich).

2.4.2 Media Selection Process

Initially, the seeding conditions for spheroid formation were carried out with 7,500 cells per well as previously described and the well plate was then incubated overnight at 37°C with 5% CO_2. The following day, the media in each well plate was carefully removed and replaced with 100 µL of each culture mediums (CO_2 independent medium, Hibernate A medium and Hibernate E medium). The well plates were then placed in sterile bags (Eline) to maintain sterility and incubated at room temperature for 3 days.

2.5 Viability Assay

Three days after room temperature incubation, the media in each well was carefully discarded. Then, an equal volume of CellTiter-Glo 3D reagent (Promega) to NGM was mixed, and 100 µL of this mixture was added to each well plate, ensuring that the procedure was protected from light to prevent degradation of the reagent. The plate was then placed on a shaker and mixed for 5 minutes to ensure proper mixing of the reagent. Following this, the plate was incubated at room temperature for 25 minutes to allow the luminescent signal to stabilize. Subsequently, the contents of each well were quickly transferred to opaque-walled 96 well plate (Greiner Bio-One), including one row with media and cryoprotectant as a control. Finally, the opaque-walled plate was placed in the plate reader (Multimode Plate reader, EnSpire 2300, Perkin Elmer) to measure luminescence, accurately determining cell viability.

2.6 Testing the Cryoprotectant-Media Combinations

Initially, various combinations of cell culture media and cryoprotectants were prepared by mixing CO_2-independent medium with 5%, 10%, and 15% concentrations of cryoprotectants. Spheroid formation was performed according to previously established protocols with 7,500 cells per well, and the plates were incubated overnight at 37°C with 5% CO_2. The following day, the media in each well was carefully aspirated and replaced with 100 µL of the prepared media-cryoprotectant mixtures.

As before, the plates were sealed in sterile Eline bags and incubated at room temperature for 3 days. Following this incubation, cell viability was assessed using the previously described viability assay protocol with CellTiter-Glo 3D reagent.

2.7 Optimizing Cryoprotectant-Media Combinations for Spheroid Viability During Freezing and Thawing

A total of 7,500 cells were seeded to form spheroids following the established protocol. These spheroids were incubated at 37°C with 5% CO_2 for three days. On Day 3, cryoprotectant-media combinations were prepared by mixing CO_2-independent medium with Nutrifreeze in concentrations of 20%, 25%, 30%, 35%, and 40%. The spheroids were transferred to cryotubes using a 100 µL pipette with the tip cut by 3-4 mm to widen the opening, allowing for gentle handling of the spheroids. Three spheroids were placed in each cryotube. Subsequently, 1,000 µL of the cryoprotectant-media combinations were added to each cryotube. The cryotubes were quickly placed in a cell freezing container (Corning) and stored in a -80°C freezer overnight. The following day, the cryotubes were transferred to a nitrogen tank at -196°C, where they were preserved for three days.

The cryotubes were taken from the nitrogen tank and quickly placed in a water bath for 3-4 minutes to thaw. The viability assay was performed with CellTiter-Glo 3D reagent immediately following the thawing of the spheroids, as previously described.

2.8 Evaluation of Enzymatic Solutions for Spheroid Dispersion

2.8.1 Hoechst Staining

A staining solution was prepared by mixing Hoechst H33342 (Invitrogen, Thermo Fisher Scientific) with NGM in a 1:100 ratio, followed by vortexing. The solution was kept protected from light throughout the process. After the spheroids were formed (day 0), as described before, the plates were incubated overnight. The following day (day 1), the media in each well was carefully removed, and 100 µL of staining solution was added to each well. The plates were then incubated for 20 minutes.

Following incubation, the staining solution was discarded, and the cells were washed with PBS. This procedure was repeated on days 2 and 3, after the spheroids had been incubated for 2 and 3 days, respectively.

2.8.2 Enzymatic Treatment

Two enzymatic solutions, Trypsin and Accutase (Thermo Fisher Scientific), were evaluated for their effectiveness in spheroid dispersion. Trypsin, widely used for cell detachment, exhibits strong enzymatic activity but can degrade cell surface markers. Accutase, on the other hand, offers a milder enzymatic action, allowing for efficient detachment while better preserving cell surface proteins [77].

After the spheroids were stained, 100 µL of each enzymatic solution was separately added to each well plate, with each well receiving the solution. The enzymatic solution was first applied and allowed to disperse the spheroids for 10 minutes. After this time, the cell suspensions were diluted 5 times in media and immediately imaged under a microscope. This process was also repeated with dispersion times of 20 minutes and 30 minutes, followed by microscopy. The entire procedure was carried out at 24-, 48-, and 72-hours post-spheroid formation.

2.8.3 Fluorescence Imaging Analysis of Spheroids

Fluorescence imaging analysis was conducted using a LifeCell Olympus IX83 automated fluorescence microscope (Olympus) with CellSense Dimensions software. Initially, the well plate was calibrated using the well navigator. The position of each spheroid was set manually. Imaging was performed with the DAPI filter, an exposure time of 600 ms, and a Lumencor Spectra X lamp set to 41%. The live frame rate was set to 10 fps. The placement of each spheroid was determined manually.

2.9 Cryopreservation and Re-cultivation of Spheroids in Cryotube

The cryotube was first coated with the FLEX coating solution for 3 minutes, then the solution was discarded, and the cryotube was incubated at room temperature under a laminar flow hood for 30 minutes. Following this, 7,500 cells were seeded into the cryotube with CO_2-independent medium supplemented with 10% FBS and 1% antibiotic. The cryotubes were then centrifuged at 1200 rpm for 5 minutes and incubated for 3 days at 37°C with 5% CO_2.

After the incubation period, the medium in each cryotube was replaced with CO_2-independent medium containing 15% and 30% NutriFreez, followed by overnight storage at -80°C.

The next day, the cryotubes were transferred to a nitrogen tank at -196°C for three days. After storage, they were thawed by immersion in a 37°C water bath for 3–4 minutes and then immediately transferred to an incubator. For each condition, two cryotubes were used, one for a viability assay and the other for re-cultivation. The viability assay and re-cultivation were conducted at three distinct time points: immediately after thawing (Phase 1), 24 hours post-thaw in incubation at 37°C (Phase 2), and 48 hours post-thaw at room temperature (Phase 3), as demonstrated in Figure 18.

The viability was measured by CellTiter-Glo 3D reagent according to the previous protocol. For spheroid re-cultivation, the medium in each cryotube was discarded, and the cells were treated with 100 µL of Trypsin for 5 minutes. Afterward, Trypsin was neutralized with 1 mL of NGM, and the cell suspension was transferred to a 48-well plate.

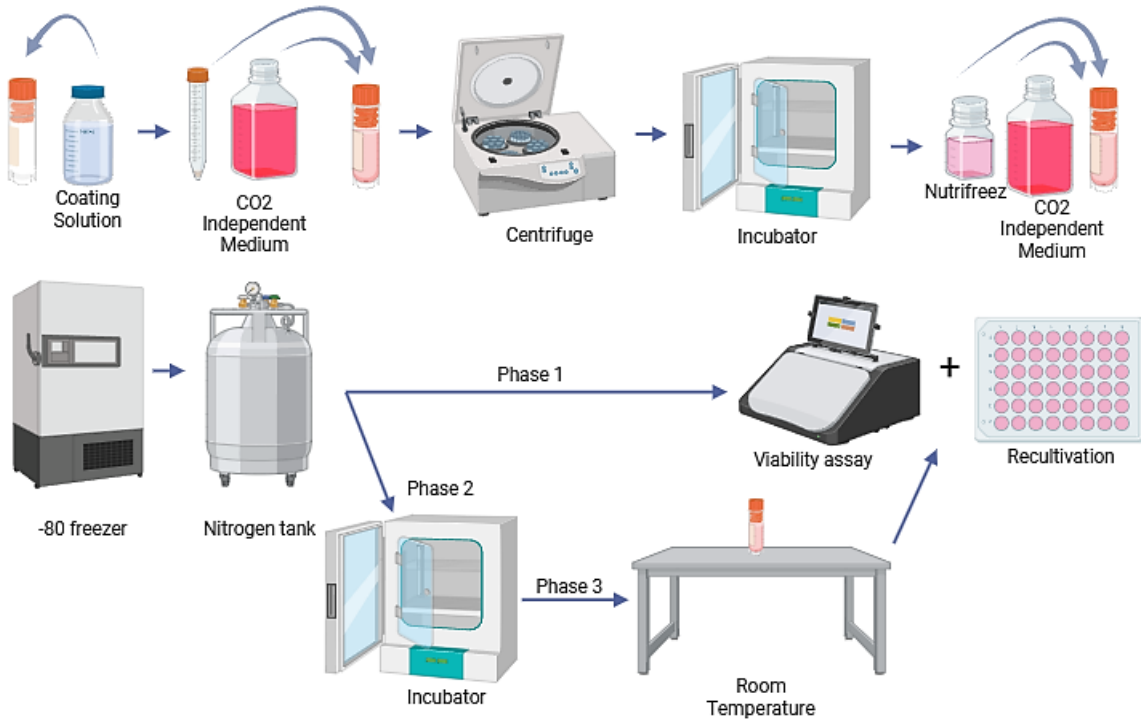

Figure 18. Procedure for cryopreservation and re-cultivation of spheroid in cryotube, created with BioRender.com

2.10 Transfreez Cryotube Insert (Cryoinsert)

2.10.1 Prototyping Device

The Cryoinsert was designed using Autodesk Fusion 360 software (Autodesk). It was engineered to fit within a cryotube, with a diameter of 10 mm and a height of 5 mm. facilitate spheroid formation, the design included 19 tiny holes, each measuring 1.5 mm in diameter and 1.5 mm in height, allowing for precise cell placement. After the design process, the file was exported in. stl format for subsequent project phases.

Figure 19. Rendor of Transfreez cryotube insert

2.10.2 Printing Phase

The Asiga Max X43 3D printer (Asiga) was used for the fabrication process, with all steps conducted in a UV-protected environment. First, the resin levels were checked and refilled as needed. The resin used was Asiga PlasClear, which enables the printing of transparent inserts suitable for microscopy. First, the .stl files were loaded into the slicing software, Asiga Composer (Asiga), to facilitate layer-by-layer construction. The printers build plate was altered by adding Arcare 92712 double adhesive tape. On the tape one liner was left in place to accomplish a smooth surface on the printer's build plate. Through this adaptation a smooth, clear attachment side can be achieved on the printed part. The print settings were configured with an addition of an approximately 3x longer burn in from the recommended first layer exposure time, thus ensuring propper first layer adhesion. Various layer heights and exposure times were adjusted, to reduce printing time while ensuring limited layer lines in essential parts of the print.

As a printing parameter, a layer height of 10 µm was used for cell structures to ensure precision and detail, while the bulk material was printed with a layer height of 100 µm to optimize printing efficiency. After setting these parameters, the model was loaded into the printer, and the printing process commenced.

2.10.3 Post-Processing Phase

After printing, the insert was carefully removed from the build platform and immersed in 70% ethanol to remove any excess resin on its surface. This was followed by placing the insert in an ultrasonic bath (VWR) for several minutes to further eliminate residual resin, and it was then exposed to compressed air. Following this, the printed Cryoinsert was placed in a Form Cure (Formlabs) at 60°C for one hour to solidify the resin.

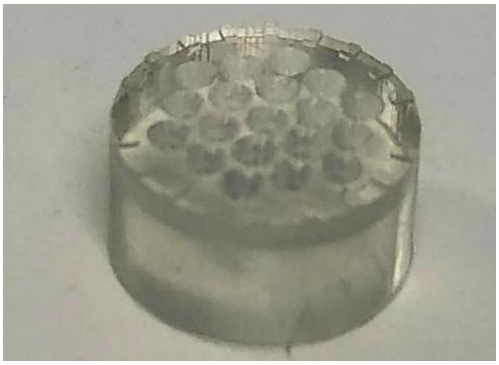

Figure 20. 3D printed Transfreez cryotube insert

2.11 Testing the Suitability of Cryoinsert Device

To test the suitability of the Cryoinsert, the insert was placed in a well of a 48-well plate and washed three times with 70% ethanol, followed by five washes with a PBS solution containing 1% antibiotic. The insert was then coated with the FLEX coating solution as previously discussed. Subsequently, 10,000 cells were seeded on each insert, treated with NGM (supplemented with 10% FBS and 1% antibiotic), and incubated at 37°C with 5% CO_2 for three days. After incubation, the cells were examined using a cell culture microscope.

2.12 Evaluation of Cryoinsert Applicability

To evaluate the applicability of the Cryoinsert, it was first washed as previously described. After placing it in a cryotube, the Cryoinsert was coated with the FLEX coating solution for 3 minutes. The coating solution was then discarded, and the insert was incubated at room temperature for 30 minutes. Subsequently, 10,000 cells were seeded onto the Cryoinsert, treated with CO_2-independent medium supplemented with 10% FBS and 1% antibiotic, and incubated for 3 days.

After incubation, the cells were treated with 15% and 30% NutriFreez in CO_2-independent medium and stored in a -80°C freezer overnight. The following day, the cryotube was transferred to a nitrogen tank at -196°C for three days before being thawed. After thawing, 200 µL of Trypsin was added to each Cryoinsert for 5 minutes, neutralized with 1 mL of media, and transferred to a 48-well plate for incubation at 37°C for 3 days.

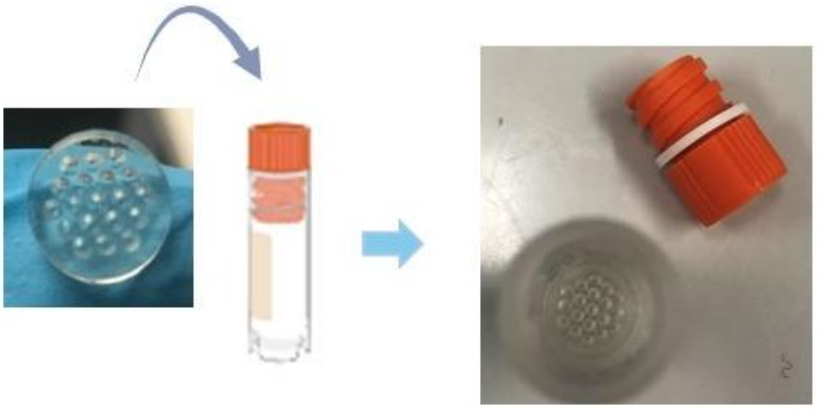

Figure 21. 3D printed cryoinsert in cryotube, created with BioRender.com

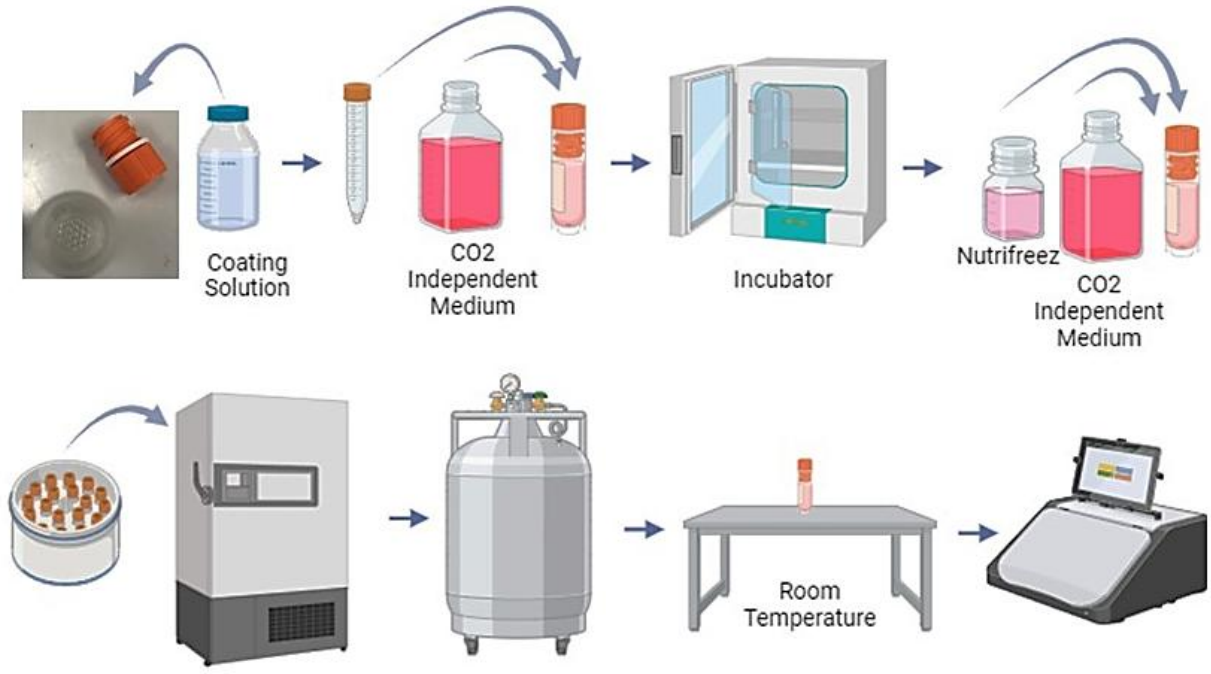

Figure 22. workflow for evaluating cryoinsert applicability, created with BioRender.com

2.13 Data Analysis

All experimental calculations were performed using Microsoft Excel, and the data was visualized through graphs created with GraphPad Prism 8.0.1 (GraphPad Software Inc.). ChatGPT by OpenAI was used to improve the clarity and flow of the text.

Fluorescent image analysis was performed using the open-source software Fiji (ImageJ). The size of spheroids, cellular aggregates, or individual cells was determined with the "Analyze" tool, following configuration of measurement parameters in the "Set Measurements" tool. Before analysis, image scales were calibrated using the provided scale bar, setting units to micrometers.

To assess the effectiveness of enzymatic solutions in spheroid dispersion, particle sizes were quantified in Fiji. Measurements were limited to areas between 100 µm², representing the approximate of size of a single cell, and 7000 µm² to accommodate for varying aggregate sizes. Threshold values were adjusted between 65% and 75% to ensure precise segmentation, with the exact value optimized for each image based on its specific characteristics.

Particles were categorized based on their size into three distinct groups: well-dispersed spheroids, medium aggregates, and large aggregates. Well-dispersed spheroids, with sizes ranging from 100–300 µm², are exemplified by particle 1 in the Figure 23, which has an area of approximately 114 µm², representing an individual cell. Medium aggregates, defined as particles with sizes between 300–700 µm², are represented by particle 2, which has an area of approximately 421 µm². Large aggregates, ranging from 700–7000 µm², include particle 3, with an area of approximately 1184 µm², showcasing the larger clustering of cells.

A

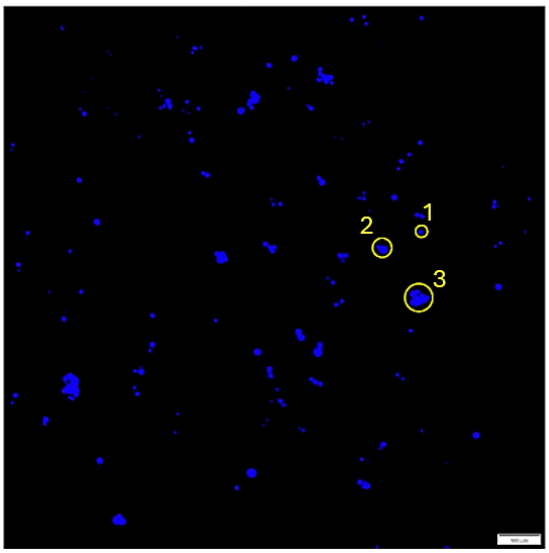

B

Results

File Edit Font Results

	Area	Mean	Min	Max
1	114.548	255	255	255
2	421.456	255	255	255
3	1184.580	255	255	255

Figure 23. (A) Fluorescence microscopy image of spheroids post-dispersion, stained with Hoechst, highlighting particles analyzed for size. (B) Size measurement results from FIJI software, categorizing Particle 1 (114 µm²) as well-dispersed spheroids, Particle 2 (421 µm²) as a medium aggregate, and Particle 3 (1184 µm²) as a large aggregate.

3. Results

3.1 Media Selection for Room Temperature Cultivation

The aim was to identify which media results in the highest cell viability after 3 days cultivation at room temperature. The results of the viability assay using the CellTiter-Glo 3D reagent, as shown in Figure 24, demonstrate the impact of different types of medium on the viability of HeLa and HEK 293 cell lines.

Figure 24, A, demonstrates that for HeLa cells, the CO_2 independent medium, which uses alternative buffering systems instead of the conventional bicarbonate CO_2 system found in standard media, demonstrated the highest cell viability, outperforming the other tested media. Hibernate A (HA) and Hibernate E (HE) mediums, which formulated for cultures outside of CO_2 environments, showed slightly lower viability but still maintained substantial cell survival. Notably, NGM (normal growth medium), which relies on standard CO_2 buffering system, resulted in the lowest viability.

HEK cells as represented in figure 24, B, the CO_2-independent medium demonstrated the highest viability, though it only marginally outperformed the other tested media. No significant differences were observed among HA, HE, and NGM, although NGM showed slightly lower viability compared to the other conditions.

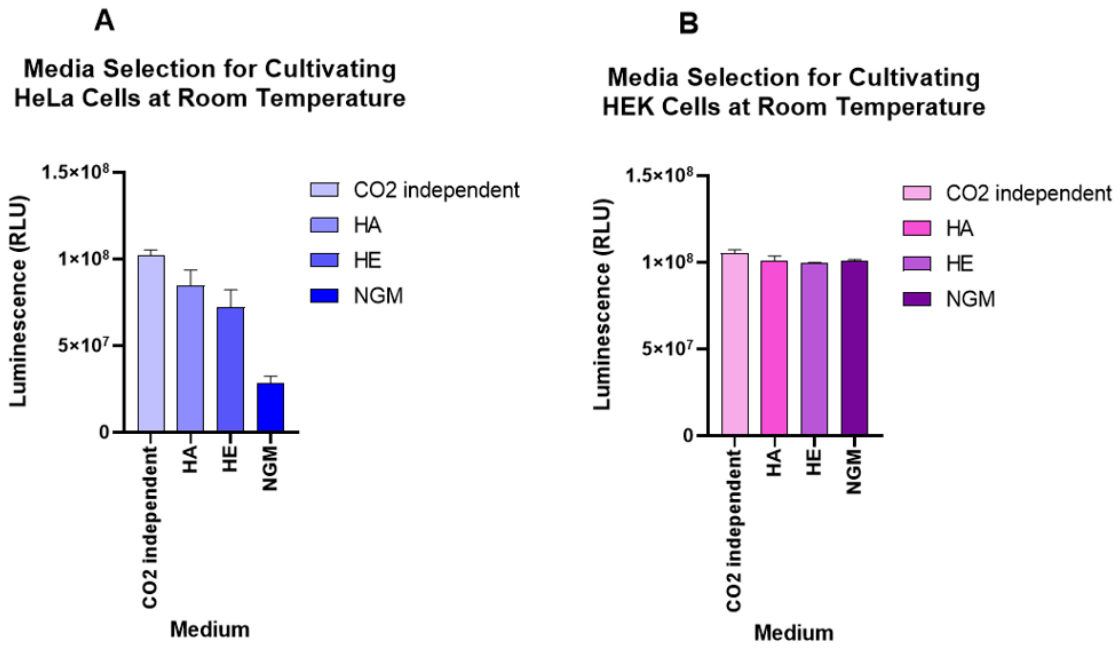

Figure 24. The cell viability for HeLa and HEK cell lines, cultured at room temperature in CO_2 independent medium, HA, HE, and NGM

3.2 Evaluation of the Effects of Various CPAs on the Cell Viability at Room Temperature Cultivation

To evaluate how different concentrations of CPA affect cell viability, NutriFreez, DMSO, and CryoSOfree were tested at 5%, 10%, and 15% in CO_2 independent medium, which had shown optimal performance at room temperature cultivation. For each test, 7,500 cells were seeded to form spheroids, incubated at 37°C with 5% CO_2. The following day, the media was replaced with CO_2 independent medium containing 5%, 10%, and 15% of each CPA and cultivated at room temperature for 3 days.

The cell viability outcomes for HEK cells across various concentrations of NutriFreez, DMSO, and CryoSOfree in CO_2-independent medium are depicted in Figure 25, A. The results indicate that, NutriFreez showed the highest cell viability at 10%, with 5% and 15% concentrations yielding slightly lower. DMSO performed best at 5%, while its 10% concentration led to reduced viability, and 15% showed the lowest results. CryoSOfree achieved optimal viability at 15%, with lower outcomes at 10% and 5%.

When comparing the overall effectiveness of the three CPAs in CO_2 independent medium, NutriFreez consistently outperformed DMSO and CryoSOfree, particularly at the 10% concentration, demonstrating the highest cell viability under comparable conditions.

The viability of HeLa cells across different concentrations of NutriFreez, DMSO, and CryoSOfree in CO_2-independent medium is presented in Figure 25, B.

NutriFreez achieved the highest viability at 10% and 15% concentrations, with the 5% concentration yielding slightly lower but comparable outcomes. DMSO demonstrated peak viability at 10%, while both the 5% and 15% concentrations resulted in decreased cell viability. Similarly, CryoSOfree showed its highest viability at 10%, with slightly lower levels at 5% and 15%. Overall, NutriFreez consistently supported higher HeLa cell viability across multiple concentrations, outperforming DMSO and CryoSOfree, particularly at the 10% concentration.

When comparing the two cell lines, HeLa and HEK, NutriFreez consistently delivered the highest viability in both, particularly at the 10% concentration. The higher overall viability of HeLa cells across all cryoprotectants and concentrations demonstrates their remarkable resilience and consistent performance. In comparison, HEK cells were more sensitive to variations in cryoprotectant conditions, showing lower viability overall and indicating that they are less resilient under the same experimental conditions.

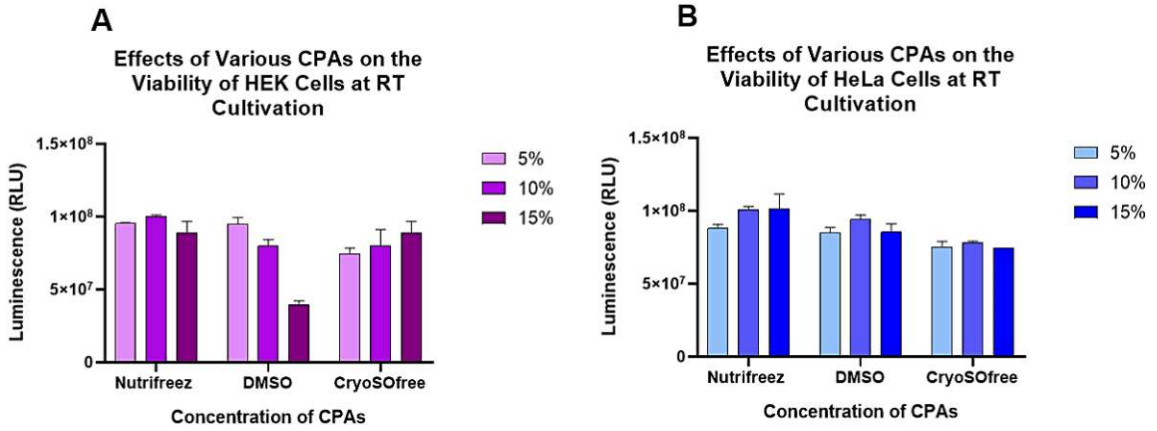

Figure 25. Evaluation of 5%, 10%, and 15% of NutriFreez, DMSO, and CryoSOfree in CO_2 independent medium on the viability of HEK cells (A) and HeLa (B) in room temperature cultivation

3.3 Optimization of CPA Concentration for Spheroid freezing

The optimization of cryoprotectant agent (CPA) concentration was evaluated using NutriFreez, which achieved the highest cell viability for both cell lines, at higher concentrations in CO_2 independent medium. Additionally, 10% DMSO was included as a gold standard for comparison, representing a widely accepted cryoprotectant benchmark in cell preservation.

Once spheroids had formed, they were treated with Nutrifreez at concentrations ranging from 5% to 40% in CO_2 independent medium, then frozen at -80°C overnight and preserved in liquid nitrogen for three days. After thawing, a viability assay was conducted immediately to assess the cryoprotection efficiency of each concentration, as represented in Figure 26.

For HEK cells the highest cell viability was observed at a 25-30% concentration of NutriFreez. As the concentration increased beyond 25%, there was a noticeable decline in viability, with a gradual decrease at 35%, and the lowest viability recorded at 40%. This indicates that for HEK cells, a concentration of 25-30% NutriFreez demonstrated comparable viability to those treated with 10% DMSO and provides the most favorable conditions for maintaining cell viability, while higher concentrations result in reduced survival.

In HeLa cells the 30% concentration of NutriFreez produced the highest viability, while concentrations beyond this point led to a significant drop in viability. At 35% and 40% the viability progressively decreased, with the lowest viability recorded at 40%. This suggests that the 30% concentration of NutriFreez produced results closest to those achieved with the 10% DMSO standard, making it a highly effective alternative for HeLa cells, while higher concentrations have a detrimental effect on their survival.

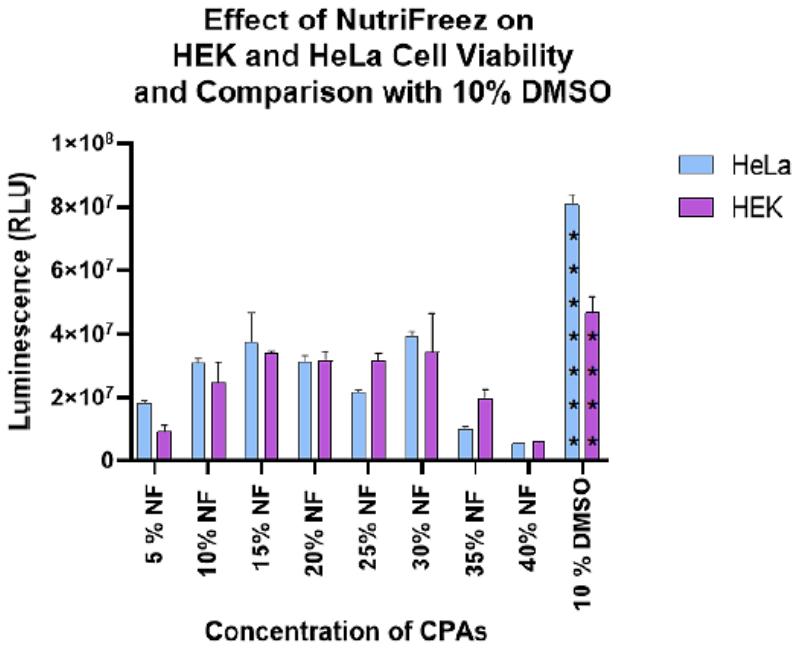

Figure 26. Optimization of cryoprotectant agent (CPA) concentration for HEK and HeLa cells, representing cell viability for HEK and HeLa cells at varying concentrations of NutriFreez in a CO2 independent medium and 10% DMSO as standard condition for cryopreservation

Generally, the optimization of NutriFreez concentrations revealed that both HEK and HeLa cells achieved their highest viability at a concentration of 30%, with a decrease in viability observed at higher concentrations. Nonetheless, both cell lines experienced the lowest viability at 40%, indicating that excessive NutriFreez concentrations are detrimental to cell survival.

3.4 Analysis of Enzymatic Solutions for Spheroid Dispersion

To evaluate the effectiveness of enzymatic solutions for spheroid dispersion they were first stained with Hoechst (H33342), after which Trypsin and Accutase were assessed for their effectiveness in dispersing the spheroids at 1-, 2-, and 3-days post-formation. The enzymatic solutions were added to the well plates, and dispersion times were set at 10, 20, and 30 minutes for evaluation. After each interval, the spheroids were immediately imaged under a fluorescence microscope. For the evaluation of spheroid size, aggregates measuring 100-300 µm² were classified as well-dispersed spheroid, those between 300-700 µm² as small aggregates, and those between 700-7000 µm² as large aggregates. The observation of aggregates within the 100–300 µm² range indicates successful dispersion, with aggregates fully dissociated into smaller components.

Dispersion outcomes and the varying degrees of enzymatic effectiveness are visually represented in Figure 27. Panel A depicts the condition where most dispersed particles are within the 100–300 µm² range, indicating successful enzymatic digestion. Panel B shows a condition dominated by medium aggregates, with particle sizes ranging from 300–700 µm², reflecting partial dispersion where some cells remain clustered. Panel C highlights a condition with the majority of particles in the 700–7000 µm² range, signifying insufficient enzymatic dispersion and incomplete breakdown of spheroids. These images demonstrate the effectiveness of the enzymatic solutions under different treatment conditions.

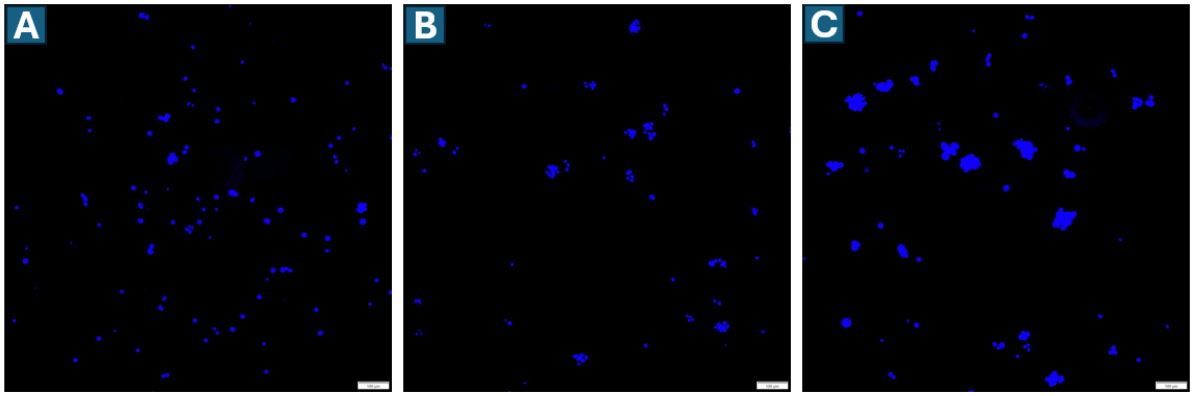

Figure 27. Visual representation of spheroid dispersion. (A) Majority of particles in the 100–300 µm² range, indicating good dispersion of spheroids. (B) Predominantly medium aggregates (300–700 µm²), reflecting partial dispersion. (C) Large aggregates (700–7000 µm²), indicating incomplete enzymatic breakdown of spheroids. 200 µm scale bar

3.4.1 Spheroid Dispersion 24 Hour Post-Formation

In HEK cells, Trypsin treatment produced consistently higher counts of well-dispersed spheroids (100–300 µm²) across all time points, with a peak observed at 10 minutes, as shown in Figure 28, A. In contrast, Accutase generated fewer well-dispersed spheroids and retained more large aggregates, indicating lower overall dispersion efficiency compared to Trypsin. Overall, Trypsin was more effective for HEK spheroid dispersion within the 24-hour time frame.

In HeLa cells, Accutase consistently produced higher counts of well-dispersed spheroids across all three time points compared to Trypsin. Trypsin, on the other hand, exhibited higher levels of medium aggregates (300–700 µm²) at all time points. Both enzymes achieved their peak well-dispersed spheroid counts at 10 minutes (Trypsin) and 30 minutes (Accutase), as illustrated in Figure 28, B.

In summary, HEK spheroids displayed greater sensitivity to Trypsin, particularly in generating well-dispersed spheroids, while HeLa spheroids responded more effectively to Accutase within the same time frame.

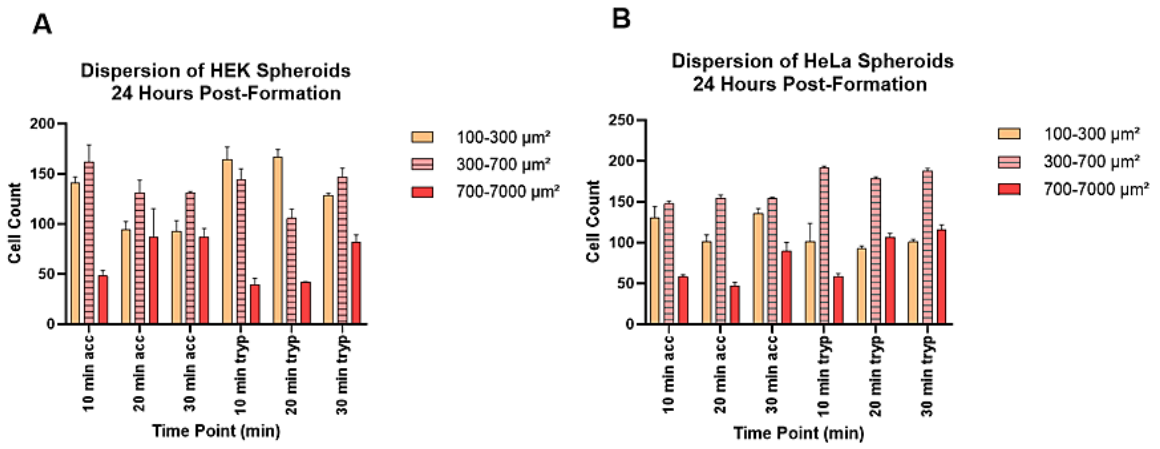

Figure 28. Comparison of Accutase and Trypsin in Dispersing HEK (A) and HeLa (B) spheroids 24 hours post-formation, evaluated at 10, 20, and 30 minutes

3.4.2 Spheroid Dispersion 48 Hour Post-Formation

For HEK cells, the comparison between Accutase and Trypsin revealed that both enzymes resulted in a significant presence of large aggregations (700–7000 µm²) at 48 hours post-formation, as visualized in Figure 29, A. At the 30-minute time point, Accutase produced a higher number of large aggregations, indicating its reduced efficiency in fully dissociating spheroids. In contrast, Trypsin generated a higher level of well-dispersed spheroids (100–300 µm²) at the same time point, suggesting its relatively better performance in breaking spheroids into individual units.

For HeLa cells, a similar trend was observed, with large aggregations being highly prominent, while the production of well-dispersed spheroids remained notably low as detailed in Figure 29, B. This consistency across all conditions highlights the reduced efficiency of both Accutase and Trypsin in dissociating HeLa spheroids on the second day post-formation.

Compared to the results observed 24 hours post-formation, both HEK and HeLa cells showed a significant decrease in single-cell generation, accompanied by a marked increase in large aggregations. This shift emphasizes the increasing resistance of HeLa and HEK spheroids to enzymatic digestion at 48 hours post-formation.

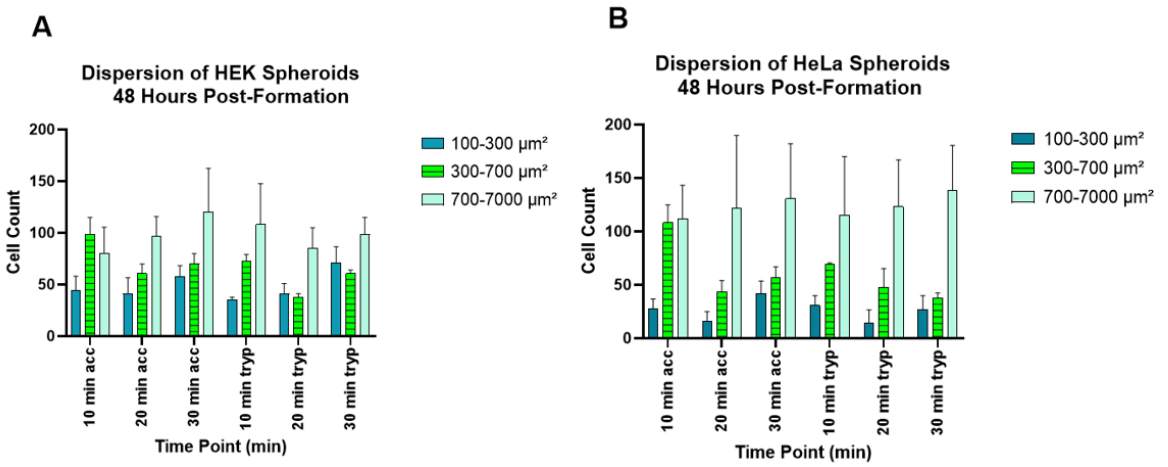

Figure 29. Comparison of Accutase and Trypsin in Dispersing HEK (A) and HeLa (B) spheroids 48 hours post-formation, evaluated at 10, 20, and 30 minutes

3.4.3 Spheroid Dispersion 72 Hour Post-Formation

In HEK cells, a comparison between Accutase and Trypsin at 72 hours post-formation revealed that Accutase consistently produced a higher number of well-dispersed spheroids (100–300 µm²) across all time intervals (10, 20, and 30 minutes) compared to Trypsin as evidenced in Figure 30, A**.** Additionally, large aggregations (700–7000 µm²) and medium aggregations (300–700 µm²) remained relatively stable across all time points, with no significant differences observed between the two enzymes, suggesting similar performance in breaking spheroids into intermediate and large sized clusters.

In HeLa cells, Trypsin produced a higher number of medium aggregations compared to Accutase, indicating less effective dissociation into well-dispersed spheroids as shown by Figure 30, B. Conversely, Accutase demonstrated superior performance in generating well-dispersed spheroids at 20 minutes. For Trypsin, the peak single-cell count occurred earlier, at the 10-minute mark.

Across both HEK and HeLa spheroids, there was a marked decrease in the level of large aggregations compared to the previous day (48 hours post-formation), alongside an increase in well-dispersed spheroids counts. This trend indicates an enhanced sensitivity of spheroids to enzymatic treatments 72 hours after seeding. HeLa spheroids exhibited greater sensitivity to enzymatic digestion than HEK spheroids.

This was evident from the lower peak aggregation levels observed in HeLa cells, with a larger proportion dissociating into well-dispersed spheroids. In contrast, HEK spheroids retained more large aggregations, demonstrating greater resistance to enzymatic digestion.

Overall, at 72 hours post-formation, HeLa spheroids displayed higher susceptibility to enzymatic dispersion compared to HEK spheroids. These findings underscore the importance of selecting the appropriate enzyme and optimizing the timing of treatment based on cell type and the stage of spheroid formation.

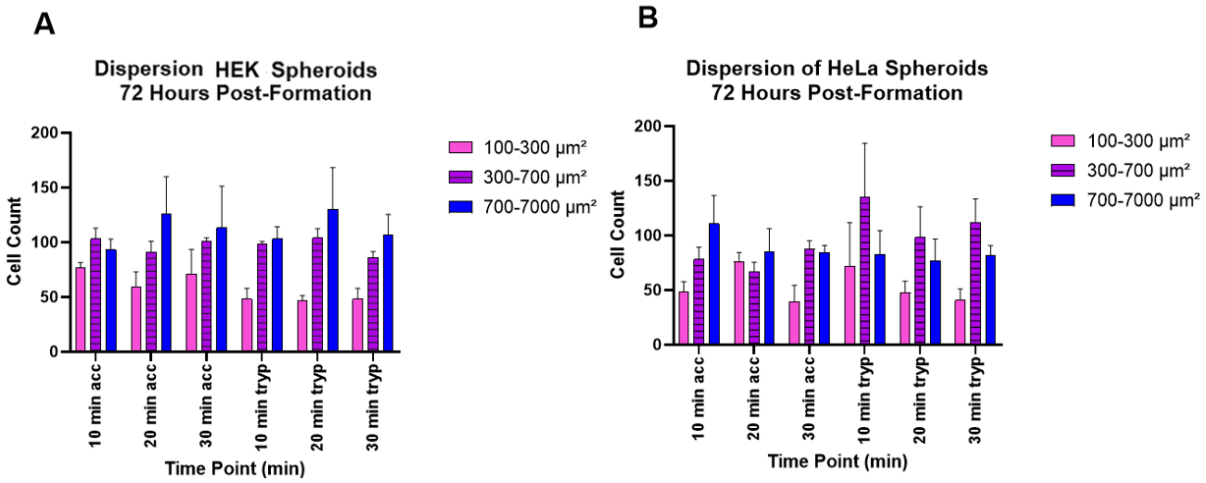

Figure 30. Comparison of Accutase and Trypsin in Dispersing HEK (A) and HeLa (B) spheroids 72 hours post-formation, evaluated at 10, 20, and 30 minutes

When comparing dispersion efficiency across all time points, Day 1 (24 hours post-formation) proved to be the most effective for generating well-dispersed spheroids in both HEK and HeLa cells. Trypsin performed best for HEK spheroids, achieving peak dispersion at 10 and 20 minutes, while Accutase was optimal for HeLa spheroids at 10 and 30 minutes. By Day 2 (48 hours post-formation), resistance to enzymatic digestion increased in both cell lines, resulting in more large aggregates and fewer well-dispersed spheroids. On Day 3 (72 hours post-formation), HeLa spheroids remained more responsive to enzymatic treatments than HEK spheroids, but overall dispersion efficiency continued to decline due to persistent large aggregates.

These results highlight Day 1 as the optimal time point for enzymatic dispersion, with Trypsin and Accutase demonstrating cell-line-specific efficacy.

3.5 Viability Assessment of Cells in Cryotube After Cryopreservation with NutriFreez

Spheroids were formed in well plates over three days and subsequently transferred to cryotubes containing CO_2-independent medium supplemented with 15% and 30% NutriFreez, as illustrated in Figure 31. The spheroids were then cryopreserved. Post-thaw, their viability was assessed using the CellTiter-Glo 3D assay, followed by recultivation across three distinct phases: immediately after thawing, after 24 hours of incubation at 37°C (24-hour post-thaw), and after an additional 24 hours of cultivation at room temperature (48-hour post-thaw).

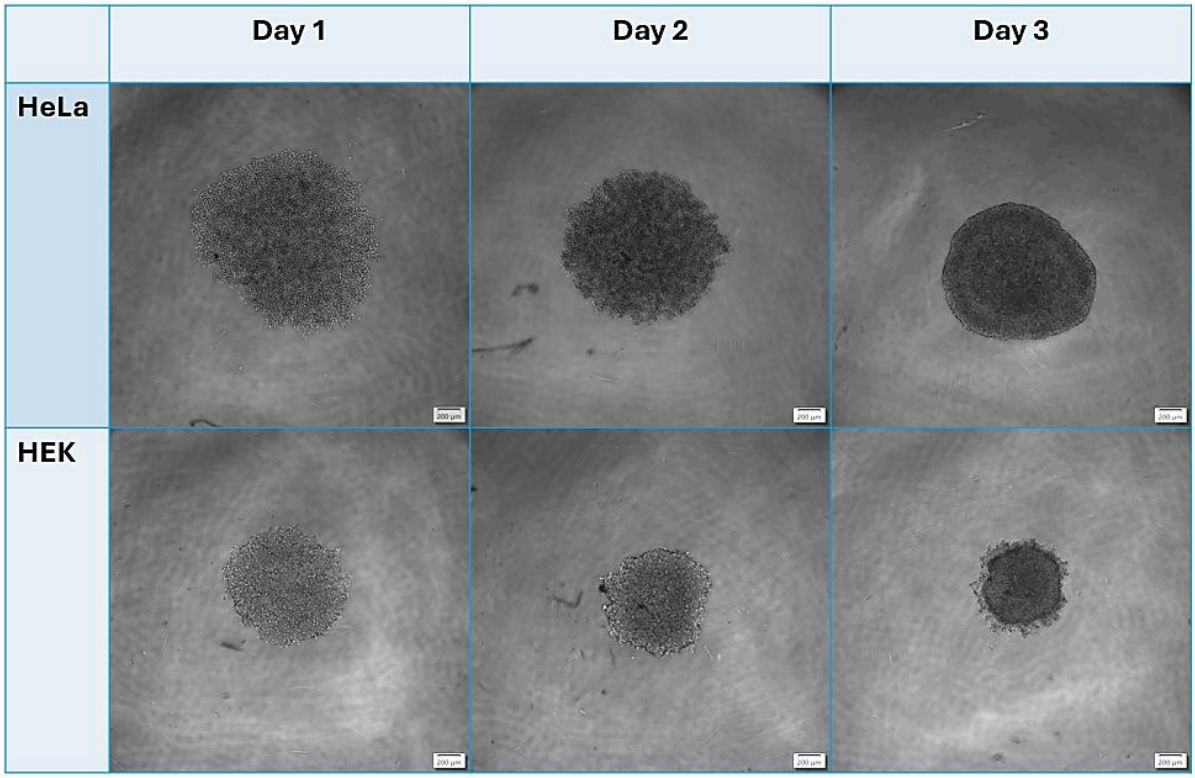

Figure 31. Spheroid formation in HEK and HeLa cells over a 3-day period. Day 1 images show initial compact spheroid structures for both cell lines. By Day 3, spheroids appear more dense and well-defined in both cell line, Scale bar: 200 µm

3.5.1 Immediate Post-Thaw

The CellTiter-Glo 3D viability assay revealed significant differences in cell survival between the two cell lines and the NutriFreez concentrations. HeLa cells treated with 30% NutriFreez demonstrated the highest viability, whereas those treated with 15% NutriFreez showed reduced viability. In contrast, HEK cells exhibited extremely low viability under both conditions, with the Luminescence values near zero, as shown in Figure 32, A.

Spheroids treated with 15% and 30% NutriFreez after freezing and re-cultivation displayed relatively cohesive structures, though some reduction in density and signs of disintegration were observed, which indicate a partial impact from the cryopreservation process, as illustrated in Figure 32, B-E.

Microscopic images captured three days after digestion, re-cultivation, and incubation of spheroids at 37°C with 5% CO_2, reveal that HeLa cells treated with 30% NutriFreez exhibited a higher density of well attached, viable cells with healthy morphology, as shown in Figure 32 (F-I). In comparison, HeLa cells treated with 15% NutriFreez exhibited fewer attached cells. HEK cells, irrespective of the NutriFreez concentration, appeared low survival and attachment rates.

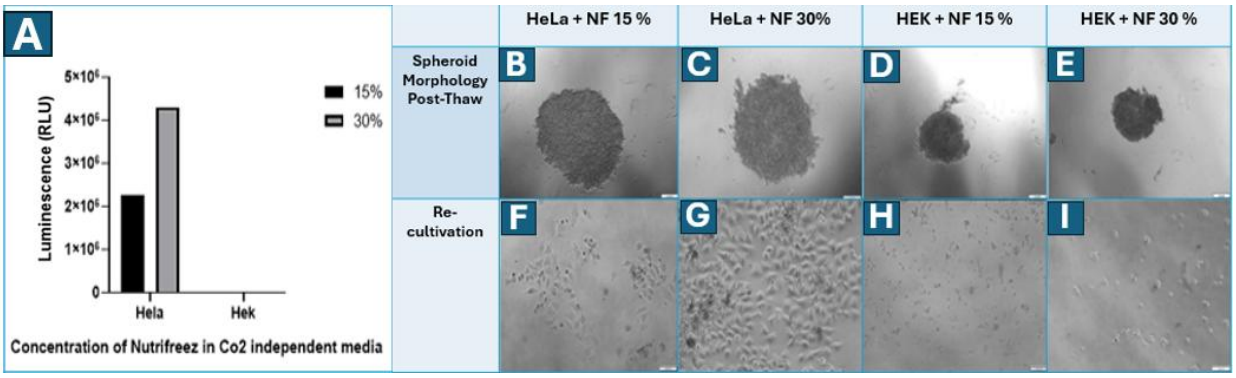

Figure 32. (A) Viability of HeLa and HEK cells following cryopreservation with 15% and 30% NutriFreez immediately post-thaw. (B, C, D, E) HeLa and HEK cells immediately post-thaw with 15% and 30% NutriFreez. (F, G, H, I) Microscopic images of HeLa and HEK cells after 3 days of incubation following digestion and re-cultivation. 200 µm scale bar

3.5.2 24-Hour Post-Thaw (37°C Incubation)

Cell viability of HeLa and HEK spheroids was evaluated 24 hours post-thaw after incubation at 37°C with 5% CO_2. The results indicate overall low survival rates for both cell lines; however, HeLa cells displayed marginally better viability, particularly at 30% NutriFreez, compared to HEK cells, which showed minimal viability at both tested concentrations, as illustrated in Figure 33, A.

Spheroids treated with 15% and 30% at 24 hour post thaw, retained a mostly intact structure but showed signs of reduced density and slight fragmentation, as depicted in Figure 33, B-E. Microscopic images (Figure 33, F-I) captured three days after digestion, re-cultivation, and incubation of spheroids at 37°C with 5% CO_2, demonstrated that across all conditions, including both 15% and 30% NutriFreez treatments for both cell lines, only unattached cells were observed. This indicates low survival across all tested conditions following cryopreservation.

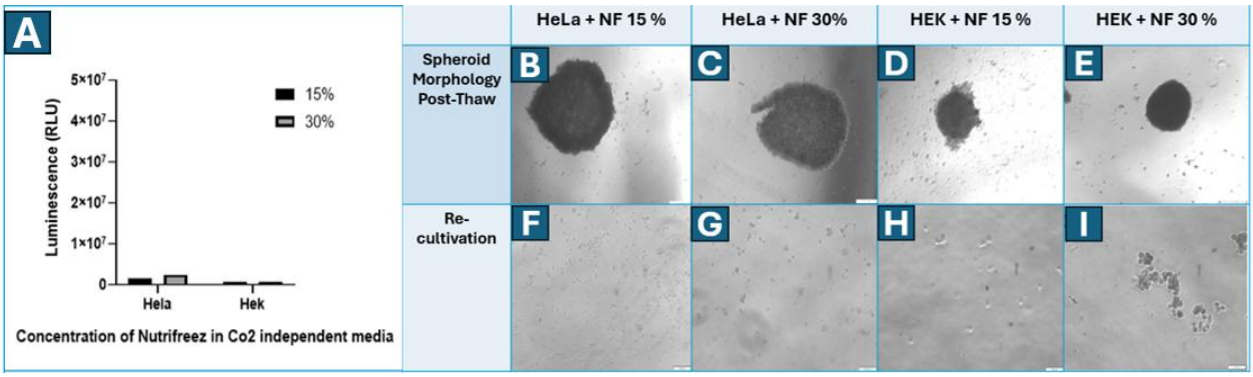

Figure 33. (A) Viability of HeLa and HEK cells following cryopreservation with 15% and 30% NutriFreez 24 Hours of Post-Thaw. (B, C, D, E) HeLa and HEK cells immediately post-thaw with 15% and 30% NutriFreez. (F, G, H, I) Microscopic images of HeLa and HEK cells after 3 days of incubation following digestion and re-cultivation. 200 µm scale bar

3.5.3 48-Hour Post-Thaw (Room Temperature)

Cell viability of HeLa and HEK spheroids was evaluated after a 48-hour post-thaw period at room temperature, as depicted in Figure 34, A. Both cell lines demonstrated low overall viability, with HeLa cells showing slightly higher viability, particularly at 30% NutriFreez. In contrast, HEK cells exhibited minimal viability at 30% and nearly none at 15%.

Morphology of spheroids treated with 15% and 30% NutriFreez 48-hour post-thaw are illustrated in Figure 34, B-E. While the spheroids retained a cohesive structure, signs of reduced density and structural damage were more pronounced compared to the 24-hour post-thaw.

Microscopic images (Figure 33, F-I) captured three days after digestion, re-cultivation, and incubation of spheroids at 37°C with 5% CO_2, revealed that, under all tested conditions, including 15% and 30% NutriFreez treatments for both cell lines, only non-attached cells were observed which indicates consistently poor survival rates across all conditions.

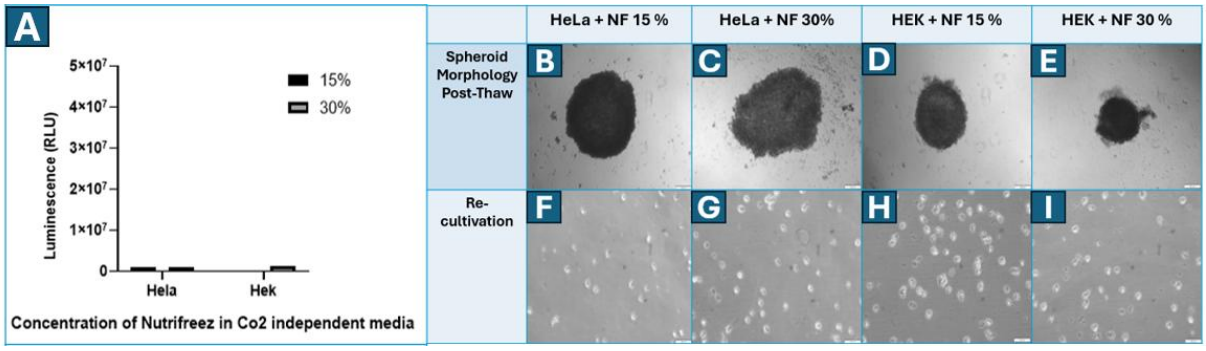

Figure 34. (A) Viability of HeLa and HEK cells following cryopreservation with 15% and 30% NutriFreez 48 Hours of Post-Thaw. (B, C, D, E) HeLa and HEK cells immediately post-thaw with 15% and 30% NutriFreez. (F, G, H, I) Microscopic images of HeLa and HEK cells after 3 days of incubation following digestion and re-cultivation. 200 µm scale bar

3.6 Evaluating the Effectiveness of Alpha Prototype Cryoinsert Device

To evaluate the feasibility of a cryotube-based system for spheroid formation, a prototype CryoSphere device was developed as demonstrated in Figure 35, A. The design includes wells at the bottom of a 3D-printed insert, specifically engineered to support spheroid formation and maintain their structural integrity. While the concept includes a stabilization mechanism to secure spheroids during transportation, this feature was not included in the initial experiments as the transportation process was simulated by room temperature incubation. Instead, the focus was placed on the efficacy of Cryoinsert.

The Cryoinsert was designed and printed to integrate effectively into standard cryotubes, and a transparent bottom was included to allow for direct microscopic observation of cells. To evaluate the device's suitability for spheroid formation, it was coated and seeded with cells in CO_2-independent medium. After three days of incubation, the morphology and size of spheroids were assessed microscopically, providing insights into the Cryoinsert's capacity to support and maintain three-dimensional cell structures.

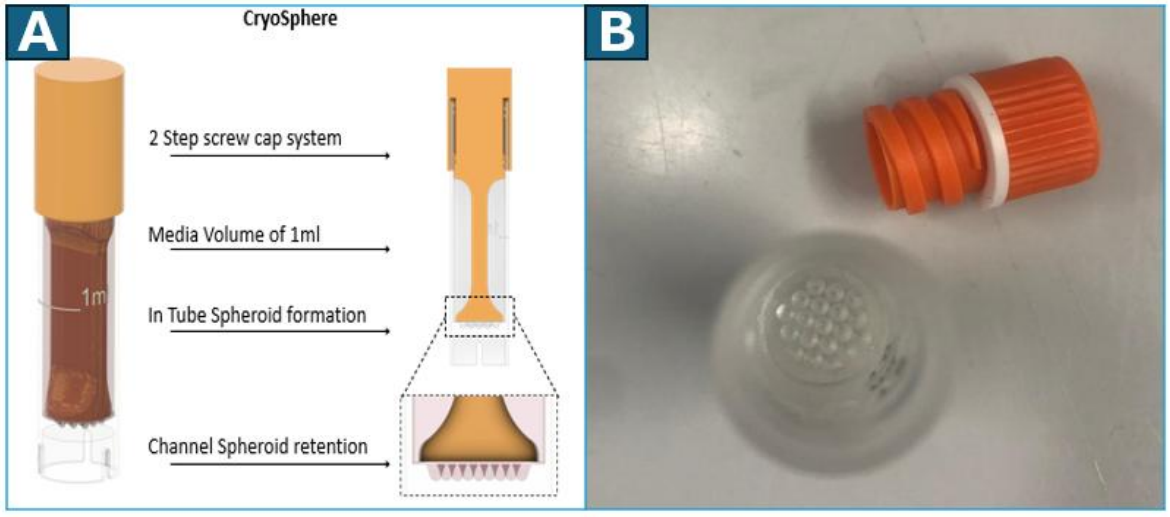

Figure 35. (A) CryoSphere device, (B) Cryoinsert placement in cryotube

Following the coating step, HeLa and HEK cells were seeded into the Cryoinsert with no leakage observed. After three days, both cell types formed well-defined spheroids measuring approximately 310 µm for HeLa and 120 µm for HEK cells (Figure 36). Despite the stepped surface texture resulting from the layer-by-layer 3D-printing process, the cells effectively agglomerated at the well bottoms, facilitating spheroid formation.

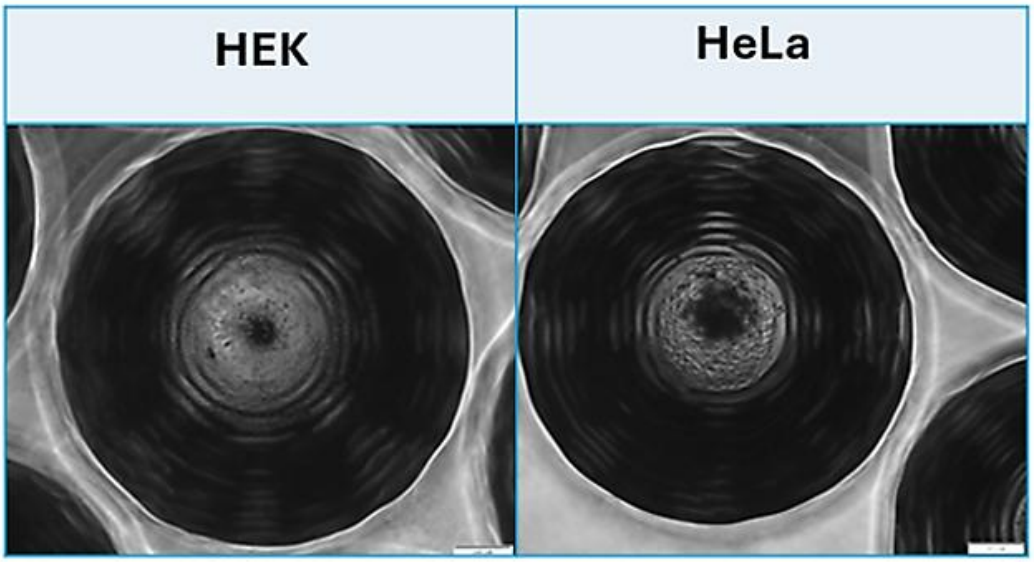

Figure 36. Formation of spheroid in cryotube insert, 200 µm scale bar

To evaluate the Cryoinsert's suitability for spheroid cryopreservation, the device was coated and seeded with HeLa and HEK cells in CO_2-independent medium. After three days of incubation, the spheroids were treated with 15% and 30% NutriFreez and cryopreserved. After thawing, spheroids were dispersed, and the cells were re-cultivated and incubated for three days at 37°C with 5% CO_2. Then the cells were examined microscopically, as shown in Figure 37.

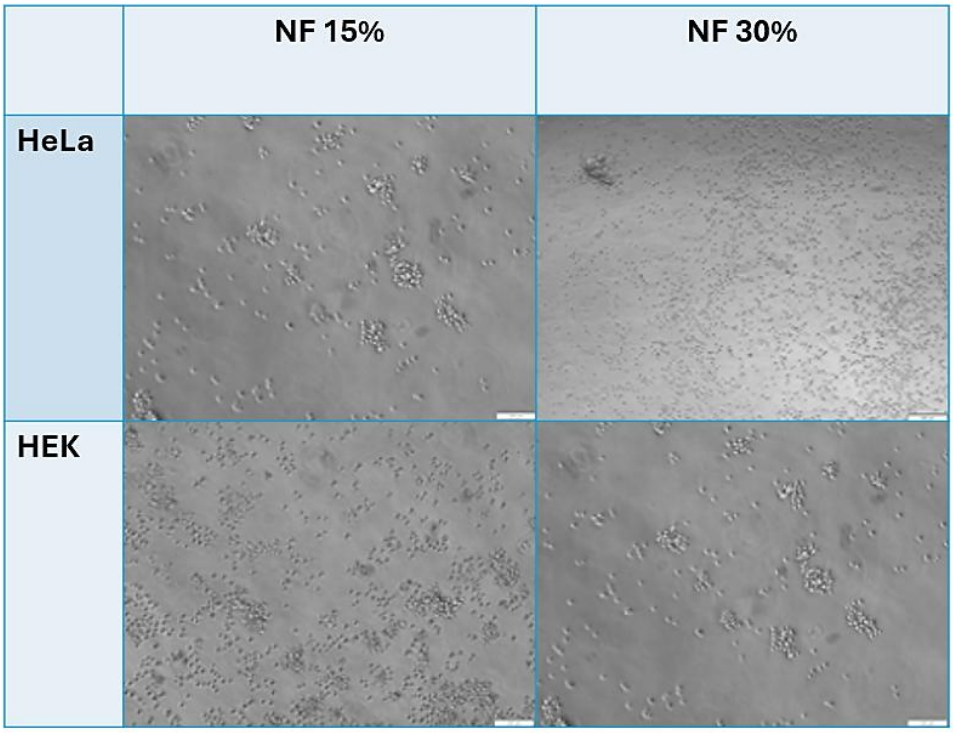

Figure 37. Microscopic images of HeLa and HEK cells post-cryopreservation with 15% and 30% NutriFreez and recultivation, 200 µm scale bar

4. Discussion & Conclusion

This thesis presents the development, optimization, and validation of a Cryoinsert system designed for the formation, cryopreservation and transportation of spheroids with targeting two of the most widely utilized cells in cell biology research, HeLa and HEK cell lines [78]. By systematically testing individual sections of the preparation and transportation workflow multiple cryoprotectant concentrations, media formulations, and enzymatic treatments, the study identified aspects essential for successful spheroid preservation and recovery.

The results of the room temperature cultivation experience demonstrate that CO_2-independent medium proved superior to other tested media, such as Hibernate A (HA), Hibernate E (HE), and the normal growth medium (NGM). This superiority may be attributed to differences in CO_2 buffering systems. However, due to the limited disclosure of ingredient information by commercial suppliers, a more precise explanation cannot be provided.

Among the tested commercial cryoprotectants for three days of room temperature cultivation, NutriFreez outperformed other cryoprotectants, including DMSO and CryoSOfree, in maintaining cell viability. While 10% DMSO is theoretically expected to provide the highest viability when freezing, cells cultivation with DMSO showed low viability, NutriFreez proved more effective, likely due to its lower DMSO content. Considering that DMSO is well-known for its toxicity, particularly at room temperature, NutriFreez emerged as the optimal alternative for cryopreservation experiments (12, 13, 16). Additionally, NutriFreez may contain other supportive ingredients that enhance cryopreservation efficiency while maintaining lower toxicity. However, the exact composition of NutriFreez is undisclosed by manufacturers, limiting a detailed understanding of its superior performance.

As NutriFreez demonstrated the highest viability at room temperature, concentrations ranging from 5% to 40% NutriFreez in CO_2-independent medium were used to preserve spheroids. A viability assay conducted immediately after thawing revealed that, for both cell lines, 15% and 30% NutriFreez showed the highest viability.

The difference in viability and cell line specific response underscores the importance of optimizing cryoprotectant conditions based on each cell type's unique characteristics, as the level of cytotoxicity during cryopreservation can vary significantly across different cell lines [79].

The higher viability and increased tolerance observed in HeLa cells under the tested conditions may be attributed to their elevated expression of heat shock proteins (HSPs), which enhance the stress resilience of HeLa cells [80, 81].

However, notable differences were observed in the digestion patterns across the three time points post-spheroid formation. At 48 hours post-formation (Day 2), spheroids exhibited fewer generated well-dispersed spheroids (100–300 μm²) and a higher proportion of large aggregations (700–7000 μm²) compared to 24 hours (Day 1) and 72 hours (Day 3).

This indicates that spheroids were more resistant to enzymatic dispersion on Day 2 than on the other tested days. This resistance may be attributed to the spheroids becoming more compact on Day 2, as observed in the experimental setup. By Day 3, the spheroids appeared to be less compact, which likely contributed to improved dissociation efficiency. From the formation of the spheroid to Day 2, all cells within the spheroid actively proliferate without any inhibited regions. During this period, nutrient and oxygen diffusion are sufficient to support cell proliferation throughout the entire structure, resulting in exponential growth. However, by Day 3, spatial gradients in nutrient and oxygen availability begin to develop.

These gradients, combined with the accumulation of metabolic waste in the core, cause cells in the central region of the spheroid to stop dividing and enter a non-proliferative state. As a result, proliferation becomes limited to the peripheral cells where nutrient and oxygen availability remain adequate. This shift leads to inhibited overall growth, marking a transition from uniform proliferation to a more stratified growth pattern dictated by the spheroid's microenvironment [82].

The extracellular microenvironment regulates cellular behavior through the arrangement and composition of the extracellular matrix (ECM) [83]. During the early stages of spheroid formation, ECM fibers act as extended connectors, cells attachments and form loose aggregates through integrin-driven interactions [84].

Treatment with Trypsin or Accutase to dissociate cells leads to the hydrolysis and removal of extracellular membrane proteins, potentially disrupting their interactions with ECM proteins [82].

This may lead to a reduction in cell-ECM interactions; however, the cells remain confined within the ECM. This entrapment could account for their heightened resistance to trypsin and accutase treatments. Employing enzymes such as collagenase, which specifically target and degrade the ECM, could offer a more effective approach to overcoming this resistance and achieving complete cell dissociation.

This study demonstrates that HeLa and HEK cell lines respond in a comparable manner to enzymatic spheroid digestion, exhibiting only slight variations in their breakdown patterns. The findings from Skog et al. (2019) align with those of the present study, showing no significant difference between Accutase and Trypsin in terms of cell viability and cell counts in keratinocytes [85].

The cryopreservation workflow was performed using cryotubes, with spheroids initially cultivated in U-bottom plates and subsequently transferred to cryotubes for cryopreservation. This approach ensured compatibility with cryogenic conditions. Two concentrations of NutriFreez, 15% and 30% in CO_2-independent medium, previously shown to result in the highest viability, were evaluated for their effects on cell viability and attachment post-thaw.

Across three phases of recultivation, distinct differences in the cryopreservation responses of HeLa and HEK cells were observed. Immediately after thawing, HeLa cells treated with 30% NutriFreez displayed significantly higher viability compared to those treated with 15% NutriFreez. This was reflected in improved cell attachment, as HeLa cells in 30% NutriFreez exhibited good attachment and confluency, while those in 15% NutriFreez were less confluent.

In contrast, HEK cells demonstrated notably lower viability across all conditions. Microscopic observations showed poor attachment and minimal recovery, regardless of the NutriFreez concentration. This highlights the inherent sensitivity of HEK cells to the cryopreservation process, even under optimized conditions.

As mentioned earlier, the higher viability and stress tolerance observed in HeLa cells could be attributed to their elevated expression HSPs, which enhance their resilience under cryopreservation conditions [80, 81].

The 24-hour post-thaw period, involving a one-day incubation at 37°C with 5% CO_2 after thawing, showed a slight increase in HEK cell viability at 30% NutriFreez, indicating that HEK cells may benefit from an overnight recovery period.

However, microscopic images of re-cultivated cells at 24-hour post-thaw revealed no attached cells and signs of morphological degradation across all conditions, indicating low overall viability. In contrast, HeLa cells were more impacted by cryoprotectant toxicity, with a notable decrease in viability, this may be attributed to post-thaw culturing in diluted DMSO, which can be problematic due to its potential toxicity [86]. Nevertheless, viability remained higher at 30% NutriFreez compared to 15%, indicating that although HeLa cells are exposed to a higher percentage of NutriFreez, which can increase toxicity, as the 30% concentration provides greater protection and efficacy during preservation, result in higher overall viability.

The 48-hour post-thaw period, which included an additional 24 hours of incubation at room temperature, demonstrated a further decline in viability for both cell lines.

This decline is likely due to extended exposure to the cryoprotectant and its associated toxicity. Compared to HEK cells, HeLa cells exhibited relatively higher viability, especially at 30% concentration. As observed in 24-Hour Post-Thaw, microscopic images of re-cultivated cells showed no cell attachment and clear signs of morphological decline across all conditions, due to the very low viability.

Microscopic images of the spheroids across all phases revealed noticeable structural deformation in each phase. This deformation is likely caused by stress from the cryoprotectant or by handling during the transfer from cryotubes to plates for imaging.

Expanding on the evaluation of spheroid cryopreservation and viability, the Alpha Prototype Cryoinsert device was analyzed for its effectiveness in supporting spheroid formation and maintaining post-thaw cell viability.

The Cryoinsert demonstrated notable success in enabling initial spheroid formation in a CO_2-independent medium, offering a reliable platform for the early stages of 3D cell culture. Both HeLa and HEK cells formed consistent spheroids, highlighting the Cryoinsert's ability to support cell aggregation and structural integrity without leakage. Additionally, the transparent bottom of the Cryoinsert allowed for direct microscopic observation of spheroid morphology, further enhancing its utility in 3D culture workflows.

The presence of resin-derived toxins made direct viability assessments, such as fluorescence imaging, unfeasible. Consequently, cells were re-cultivated to evaluate their viability post-cryopreservation.

However, when integrated into cryopreservation workflows, significant challenges became apparent. Despite successful spheroid formation and cryopreservation with 15% and 30% NutriFreez, post-thaw microscopic analysis revealed a complete absence of cell attachment and a lack of viable cells in both HeLa and HEK lines under all tested conditions.

These findings underscore two critical areas requiring improvement to enhance the functionality and efficacy of the Cryoinsert system. First, the material biocompatibility of the Cryoinsert must be addressed by optimizing the choice of resin and its curing process to minimize the leaching of toxins and create a more cell-friendly environment. Resin-derived toxins likely contributed to the lack of post-thaw viability, compromising cell survival during and after cryopreservation. Developing or selecting biocompatible materials with improved properties is essential to ensure the long-term reliability of the Cryoinsert for 3D cell culture and cryopreservation applications. Second, existing cryopreservation protocols need significant refinement to better support cell survival in conjunction with devices like the Cryoinsert. While NutriFreez was tested as a cryoprotectant, its performance under these conditions was inadequate, highlighting the need for innovative cryoprotection strategies. The development of alternative formulations with reduced toxicity and enhanced protective capabilities will be critical for improving post-thaw cell viability and attachment, enabling the Cryoinsert to realize its full potential as a versatile tool for spheroid-based research and practical applications.

In conclusion, the Cryoinsert device demonstrated significant potential as a platform for supporting spheroid formation and initial preservation, offering a promising tool for advancing 3D cell culture technologies. However, to fully realize its potential for transporting live 3D cell cultures under ambient conditions, critical challenges related to cell viability and transport must be addressed. Establishing a robust, standardized protocol for spheroid formation, cryopreservation, and transportation is paramount to ensuring consistent and reproducible outcomes.

A key step in advancing cryopreservation processes is the adoption of non-toxic cryoprotectants to replace DMSO. Novel alternatives, such as ionic liquids, deep eutectic solvents, and specialized polymers, have shown significant potential in reducing cytotoxicity while improving cell preservation during freezing and thawing. These innovative compounds offer safer and more efficient solutions for maintaining cell viability throughout the cryopreservation process [22].

Such innovations will not only enhance cell survival and viability but also mitigate the cytotoxic effects associated with traditional cryopreservation methods. By addressing these limitations, the Cryoinsert could become a reliable tool for preserving and transporting live cell cultures, paving the way for broader applications in regenerative medicine, cell-based therapies, and other cutting-edge therapeutic strategies. This progress could ultimately revolutionize the feasibility and reliability of live cell technologies, enabling transformative advancements in clinical and research settings.

5. List of References

[1] M. Busk, S. Sinning, A. K. O. Alstrup, O. L. Munk, and M. H. Vendelbo, "Nuclear Medicine Preclinical Research: The Role of Cell Cultures," (in eng), *Semin. Nucl. Med.,* vol. 53, no. 5, pp. 558-569, Sep 2023, doi: 10.1053/j.semnuclmed.2023.04.007.

[2] A. G. Souza, I. C. Ferreira, K. Marangoni, V. Bastos, and V. Goulart, "Advances in cell culture: more than a century after cultivating cells," *J. Biotechnol. Biomater,* vol. 6, no. 2, Apr 2016, Art no. 1000221, doi: 10.4172/2155-952X.1000221.

[3] F. Li, N. Vijayasankaran, A. Shen, R. Kiss, and A. Amanullah, "Cell culture processes for monoclonal antibody production," *MAbs,* vol. 2, no. 5, pp. 466-477, Sep-Oct 2010, doi: 10.4161/mabs.2.5.12720.

[4] M. N. Rahaman and J. J. Mao, "Stem cell-based composite tissue constructs for regenerative medicine," *Biotechnol. Bioeng.,* vol. 91, no. 3, pp. 261-284, Aug 2005, doi: 10.1002/bit.20292.

[5] G. Kretzmer, "Industrial processes with animal cells," *Appl. Microbiol. Biotechnol.,* vol. 59, pp. 135-142, Jul 2002, doi: 10.1007/s00253-002-0991-y.

[6] M. Butler, "Animal cell cultures: recent achievements and perspectives in the production of biopharmaceuticals," *Appl. Microbiol. Biotechnol.,* vol. 68, no. 3, pp. 283-291, Aug 2005, doi: 10.1007/s00253-005-1980-8.

[7] T. Yao and Y. Asayama, "Animal-cell culture media: History, characteristics, and current issues," *Reprod. Med. Biol.,* vol. 16, no. 2, pp. 99-117, Mar 2017, doi: 10.1002/rmb2.12024.

[8] T. A. Ponzio, H. Feindt, and S. Ferguson, "License Compliance Issues For Biopharmaceuticals: Special Challenges For Negotiations Between Companies And Non-Profit Research Institutions," (in eng), *LES Nouv.,* vol. 46, no. 3, pp. 216-225, Sep 2011. [Online]. Available: https://pmc.ncbi.nlm.nih.gov/articles/PMC3234133/.

[9] M. Ravi, V. Paramesh, S. Kaviya, E. Anuradha, and F. P. Solomon, "3D cell culture systems: advantages and applications," *J. Cell. Physiol.,* vol. 230, no. 1, pp. 16-26, Jan 2015, doi: 10.1002/jcp.24683.

[10] T. Yoshino, U. Bickham, and C. Bayne, "Molluscan cells in culture: primary cell cultures and cell lines," *Can. J. Zool.,* vol. 91, no. 6, pp. 391-404, Jun 2013, doi: 10.1139/cjz-2012-0258.

[11] P. G. Miller, Y. I. Wang, G. Swan, and M. L. Shuler, "A simple cell transport device keeps culture alive and functional during shipping," (in eng), *Biotechnol. Prog.,* vol. 33, no. 5, pp. 1257-1266, Sep 2017, doi: 10.1002/btpr.2512.

[12] S. Stefansson *et al.*, "Transporting mammalian cells at ambient temperature: A viable alternative to dry ice," *Adv. Biosci. Biotechnol.,* vol. 8, no. 4, pp. 127-133, Apr 2017, doi: 10.4236/abb.2017.84009.

[13] M. Awan *et al.*, "Dimethyl sulfoxide for cryopreservation of alginate encapsulated liver cell spheroids in bioartificial liver support; assessments of cryoprotectant toxicity tolerance and dilution strategies," *Cryobiology,* vol. 106, pp. 79-83, Jun 2022, doi: 10.1016/j.cryobiol.2022.03.007.

[14] L. Yang, C. Li, L. Chen, and Z. Li, "An agarose-gel based method for transporting cell lines," *Curr. Chem. Genomics,* vol. 3, pp. 50-53, Dec 2009, doi: 10.2174/1875397300903010050.

[15] B. N. Willbrand, S. Loh, C. E. O'Connell-Rodwell, D. O'Connell, and D. M. Ridgley, "Phoenix: A Portable, Battery-Powered, and Environmentally Controlled Platform for Long-Distance Transportation of Live-Cell Cultures," (in eng), *Front Bioeng. Biotechnol.,* vol. 8, p. 696, Jun 2020, doi: 10.3389/fbioe.2020.00696.

[16] S. Heydarzadeh, S. Kheradmand Kia, S. Boroomand, and M. Hedayati, "Recent developments in cell shipping methods," *Biotechnol. Bioeng.,* vol. 119, no. 11, pp. 2985-3006, Nov 2022, doi: 10.1002/bit.28197.

[17] O. Gryshkov *et al.*, "Coaxial alginate hydrogels: from self-assembled 3D cellular constructs to long-term storage," *Int. J. Mol. Sci.,* vol. 22, no. 6, p. 3096, Mar 2021, doi: 10.3390/ijms22063096.

[18] D. Whaley, K. Damyar, R. P. Witek, A. Mendoza, M. Alexander, and J. R. Lakey, "Cryopreservation: an overview of principles and cell-specific considerations," *Cell Transplant.,* vol. 30, pp. 1-12, Jan-Dec 2021, doi: 10.1177/0963689721999617.

[19] T. H. Jang *et al.*, "Cryopreservation and its clinical applications," *Integr. Med. Res.,* vol. 6, no. 1, pp. 12-18, Mar 2017, doi: 10.1016/j.imr.2016.12.001.

[20] T. Chang and G. Zhao, "Ice inhibition for cryopreservation: materials, strategies, and challenges," *Adv. Sci.,* vol. 8, no. 6, p. 2002425, Feb 2021, doi: 10.1002/advs.202002425.

[21] K. A. Jungare, R. Radha, and D. Sreekanth, "Cryopreservation of biological samples–A short review," *Mater. Today: Proc.,* vol. 51, no. 3, pp. 1637-1641, 2022, doi: 10.1016/j.matpr.2021.11.203.

[22] L. Lomba, C. B. García, L. Benito, E. Sangüesa, S. Santander, and E. Zuriaga, "Advances in Cryopreservatives: Exploring Safer Alternatives," *ACS Biomater. Sci. Eng.,* vol. 10, no. 1, pp. 178-190, Jan 2024, doi: 10.1021/acsbiomaterials.3c00859.

[23] M. D. Ekpo, G. F. Boafo, J. Xie, X. Liu, C. Chen, and S. Tan, "Strategies in developing dimethyl sulfoxide (DMSO)-free cryopreservation protocols for biotherapeutics," *Front. immunol.,* vol. 13, p. 1030965, Oct 2022, doi: 10.3389/fimmu.2022.1030965.

[24] J. I. Gil-Chinchilla *et al.*, "Optimizing cryopreservation conditions for use of fucosylated human mesenchymal stromal cells in anti-inflammatory/immunomodulatory therapeutics," *Front. immunol.,* vol. 15, p. 1385691, Mar 2024, doi: 10.3389/fimmu.2024.1385691.

[25] M. Kapałczyńska *et al.*, "2D and 3D cell cultures–a comparison of different types of cancer cell cultures," *Arch. Med. Sci.,* vol. 14, no. 4, pp. 910-919, Jun 2018, doi: 10.5114/aoms.2016.63743.

[26] K. Duval *et al.*, "Modeling physiological events in 2D vs. 3D cell culture," *Physiology (Bethesda),* vol. 32, no. 4, pp. 266-277, Jul 2017, doi: 10.1152/physiol.00036.2016.

[27] Y. Imamura *et al.*, "Comparison of 2D-and 3D-culture models as drug-testing platforms in breast cancer," *Oncol. Rep.,* vol. 33, no. 4, pp. 1837-1843, Apr 2015, doi: 10.3892/or.2015.3767.

[28] R. Z. Lin and H. Y. Chang, "Recent advances in three-dimensional multicellular spheroid culture for biomedical research," *Biotechnol. J.,* vol. 3, no. 9-10, pp. 1172-1184, Oct 2008, doi: 10.1002/biot.200700228.

[29] S. Nath and G. R. Devi, "Three-dimensional culture systems in cancer research: Focus on tumor spheroid model," *Pharmacol. Ther.,* vol. 163, pp. 94-108, Jul 2016, doi: 10.1016/j.pharmthera.2016.03.013.

[30] S. Gunti, A. T. Hoke, K. P. Vu, and N. R. London Jr, "Organoid and spheroid tumor models: Techniques and applications," *Cancers (Basel),* vol. 13, no. 4, p. 874, Feb 2021, doi: 10.3390/cancers13040874.

[31] M. E. Sakalem, M. T. De Sibio, F. A. d. S. da Costa, and M. de Oliveira, "Historical evolution of spheroids and organoids, and possibilities of use in life sciences and medicine," *Biotechnol. J.,* vol. 16, no. 5, p. e2000463, May 2021, doi: 10.1002/biot.202000463.

[32] S.-Y. Lee, I.-S. Koo, H. J. Hwang, and D. W. Lee, "In Vitro three-dimensional (3D) cell culture tools for spheroid and organoid models," *SLAS Discov.,* vol. 28, no. 4, pp. 119-137, Jun 2023, doi: 10.1016/j.slasd.2023.03.006.

[33] M. J. Ware *et al.*, "Generation of homogenous three-dimensional pancreatic cancer cell spheroids using an improved hanging drop technique," *Tissue Eng. Part C Methods,* vol. 22, no. 4, pp. 312-321, Apr 2016, doi: 10.1089/ten.TEC.2015.0280.

[34] L. Ferreira, V. Gaspar, and J. Mano, "Design of spherically structured 3D in vitro tumor models-Advances and prospects," *Acta Biomater.,* vol. 75, pp. 11-34, Jul 2018, doi: 10.1016/j.actbio.2018.05.034.

[35] N.-E. Ryu, S.-H. Lee, and H. Park, "Spheroid culture system methods and applications for mesenchymal stem cells," *Cells,* vol. 8, no. 12, p. 1620, Dec 2019, doi: 10.3390/cells8121620.

[36] I. Smyrek, B. Mathew, S. C. Fischer, S. M. Lissek, S. Becker, and E. H. Stelzer, "E-cadherin, actin, microtubules and FAK dominate different spheroid formation phases and important elements of tissue integrity," *Biol. Open,* vol. 8, no. 1, p. bio037051, Jan 2019, doi: 10.1242/bio.037051.

[37] H. Shen, S. Cai, C. Wu, W. Yang, H. Yu, and L. Liu, "Recent advances in three-dimensional multicellular spheroid culture and future development," *Micromachines (Basel),* vol. 12, no. 1, p. 96, Jan 2021, doi: 10.3390/mi12010096.

[38] G. Mehta, A. Y. Hsiao, M. Ingram, G. D. Luker, and S. Takayama, "Opportunities and challenges for use of tumor spheroids as models to test drug delivery and efficacy," (in eng), *J Control Release,* vol. 164, no. 2, pp. 192-204, Dec 2012, doi: 10.1016/j.jconrel.2012.04.045.

[39] T. M. Achilli, J. Meyer, and J. R. Morgan, "Advances in the formation, use and understanding of multi-cellular spheroids," (in eng), *Expert Opin. Biol. Ther.,* vol. 12, no. 10, pp. 1347–1360, Oct 2012, doi: 10.1517/14712598.2012.707181.

[40] M. Fürsatz, P. Gerges, S. Wolbank, and S. Nürnberger, "Autonomous spheroid formation by culture plate compartmentation," *Biofabrication,* vol. 13, no. 3, p. 035018, Apr 2021, doi: 10.1088/1758-5090/abe186.

[41] C. Jubelin *et al.*, "Liquid Overlay Technique allows the generation of homogeneous osteosarcoma, glioblastoma, lung and prostate adenocarcinoma spheroids that can be used for drug cytotoxicity measurements," *Front Bioeng. Biotechnol.,* vol. 11, p. 1260049, Oct 2023, doi: 10.3389/fbioe.2023.1260049.

[42] M. P. Carvalho, E. C. Costa, S. P. Miguel, and I. J. Correia, "Tumor spheroid assembly on hyaluronic acid-based structures: A review," *Carbohydr. Polym.,* vol. 150, pp. 139-148, Oct 2016, doi: 10.1016/j.carbpol.2016.05.005.

[43] M. P. Carvalho, E. C. Costa, and I. J. Correia, "Assembly of breast cancer heterotypic spheroids on hyaluronic acid coated surfaces," (in eng), *Biotechnol. Prog.,* vol. 33, no. 5, pp. 1346-1357, Sep 2017, doi: 10.1002/btpr.2497.

[44] C. Shao, J. Chi, H. Zhang, Q. Fan, Y. Zhao, and F. Ye, "Development of cell spheroids by advanced technologies," *Adv. Healthc. Mater.,* vol. 5, no. 9, p. 2000183, Jun 2020, doi: 10.1002/admt.202000183.

[45] M. C. Decarli *et al.*, "Cell spheroids as a versatile research platform: Formation mechanisms, high throughput production, characterization and applications," *Biofabrication,* vol. 13, no. 3, p. 032002, Apr 2021, doi: 10.1088/1758-5090/abe6f2.

[46] S. H. Pereira, D. S. d. M. Coutinho, A. F. d. O. G. d. Matos, W. F. d. Silva Junior, and D. L. Fabrino, "Three-dimensional cell culture, opportunities and challenges for bioprocess engineers," *Braz. J. Biol. Sci.,* vol. 3, no. 6, pp. 263-277, Jan 2016, doi: 10.21472/bjbs.030603.

[47] R. K. Vadivelu, H. Kamble, M. J. Shiddiky, and N.-T. Nguyen, "Microfluidic technology for the generation of cell spheroids and their applications," *Micromachines (Basel),* vol. 8, no. 4, p. 94, Mar 2017, doi: 10.3390/mi8040094.

[48] P. Steinwerth *et al.*, "Structural and Molecular Changes of Human Chondrocytes Exposed to the Rotating Wall Vessel Bioreactor," *Biomolecules,* vol. 14, no. 1, p. 25, Dec 2023, doi: 10.3390/biom14010025.

[49] K. Białkowska, P. Komorowski, M. Bryszewska, and K. Miłowska, "Spheroids as a type of three-dimensional cell cultures—examples of methods of preparation and the most important application," *Int. J. Mol. Sci.,* vol. 21, no. 17, p. 6225, Aug 2020, doi: 10.3390/ijms21176225.

[50] F. Leonard and B. Godin, "3D In Vitro Model for Breast Cancer Research Using Magnetic Levitation and Bioprinting Method," (in eng), *Methods Mol. Biol.,* vol. 1406, pp. 239-51, Jan 2016, doi: 10.1007/978-1-4939-3444-7_21.

[51] R. Baudoin, A. Corlu, L. Griscom, C. Legallais, and E. Leclerc, "Trends in the development of microfluidic cell biochips for in vitro hepatotoxicity," *Toxicol. In Vitro,* vol. 21, no. 4, pp. 535-544, Jun 2007, doi: 10.1016/j.tiv.2006.11.004.

[52] A. W. Chow, "Lab-on-Chip: Opportunities for chemical engineering," *AIChE Journal,* vol. 48, no. 8, pp. 1590-1595, Aug 2002, doi: 10.1002/aic.690480802.

[53] E. K. Sackmann, A. L. Fulton, and D. J. Beebe, "The present and future role of microfluidics in biomedical research," *Nature,* vol. 507, no. 7491, pp. 181-189, Mar 2014, doi: 10.1038/nature13118.

[54] Y. Temiz, R. D. Lovchik, G. V. Kaigala, and E. Delamarche, "Lab-on-a-chip devices: How to close and plug the lab?," *Microelectron. Eng.,* vol. 132, pp. 156-175, Jan 2015, doi: 10.1016/j.mee.2014.10.013.

[55] R. Pol, F. Céspedes, D. Gabriel, and M. Baeza, "Microfluidic lab-on-a-chip platforms for environmental monitoring," *TrAC - Trends Anal. Chem.,* vol. 95, pp. 62-68, Oct 2017, doi: 10.1016/j.trac.2017.08.001.

[56] S. Battat, D. A. Weitz, and G. M. Whitesides, "An outlook on microfluidics: the promise and the challenge," *Lab Chip,* vol. 22, no. 3, pp. 530-536, Feb 2022, doi: 10.1039/d1lc00731a.

[57] B. K. Nahak, A. Mishra, S. Preetam, and A. Tiwari, "Advances in organ-on-a-chip materials and devices," *ACS Appl. Bio Mater.,* vol. 5, no. 8, pp. 3576-3607, Aug 2022, doi: 10.1021/acsabm.2c00041.

[58] J. D. Caplin, N. G. Granados, M. R. James, R. Montazami, and N. Hashemi, "Microfluidic organ-on-a-chip technology for advancement of drug development and toxicology," *Adv. Healthc. Mater.,* vol. 4, no. 10, pp. 1426-1450, Jul 2015, doi: 10.1002/adhm.201500040.

[59] C. Ma, Y. Peng, H. Li, and W. Chen, "Organ-on-a-chip: a new paradigm for drug development," *Trends Pharmacol. Sci.,* vol. 42, no. 2, pp. 119-133, Feb 2021, doi: 10.1016/j.tips.2020.11.009.

[60] S. Kim and S. Takayama, "Organ-on-a-chip and the kidney," *Kidney Res. Clin. Pract.,* vol. 34, no. 3, pp. 165-169, Aug 2015, doi: 10.1016/j.krcp.2015.08.001.

[61] C. M. Leung *et al.*, "A guide to the organ-on-a-chip," *Nat. Rev. Methods Primers,* vol. 2, no. 1, May 2022, Art no. 33, doi: 10.1038/s43586-022-00118-6.

[62] S. Ahadian *et al.*, "Organ-on-a-chip platforms: a convergence of advanced materials, cells, and microscale technologies," *Adv. Healthc. Mater.,* vol. 7, no. 2, p. 1700506, Jan 2018, doi: 10.1002/adhm.201700506.

[63] Q. Ramadan and M. Zourob, "Organ-on-a-chip engineering: Toward bridging the gap between lab and industry," (in eng), *Biomicrofluidics,* vol. 14, no. 4, p. 041501, Jul 2020, doi: 10.1063/5.0011583.

[64] G. Fang, Y. C. Chen, H. Lu, and D. Jin, "Advances in Spheroids and Organoids on a Chip," *Adv. Funct. Mater.,* vol. 33, no. 19, p. 2215043, Feb 2023, doi: 10.1002/adfm.202215043.

[65] M. Rothbauer, D. Wartmann, V. Charwat, and P. Ertl, "Recent advances and future applications of microfluidic live-cell microarrays," *Biotechnol. Adv.,* vol. 33, no. 6, pp. 948-961, Nov 2015, doi: 10.1016/j.biotechadv.2015.06.006.

[66] G. Bassi, M. A. Grimaudo, S. Panseri, and M. Montesi, "Advanced multi-dimensional cellular models as emerging reality to reproduce in vitro the human body complexity," *Int. J. Mol. Sci.,* vol. 22, no. 3, p. 1195, Jan 2021, doi: 10.3390/ijms22031195.

[67] C. Eilenberger *et al.*, "A microfluidic multisize spheroid array for multiparametric screening of anticancer drugs and blood–brain barrier transport properties," *Adv. Sci.,* vol. 8, no. 11, p. 2004856, Jun 2021, doi: 10.1002/advs.202004856.

[68] D. J. Guckenberger, T. E. De Groot, A. M. Wan, D. J. Beebe, and E. W. Young, "Micromilling: a method for ultra-rapid prototyping of plastic microfluidic devices," *Lab Chip,* vol. 15, no. 11, pp. 2364-2378, Jun 2015, doi: 10.1039/c5lc00234f.

[69] C.-W. Tsao, "Polymer microfluidics: Simple, low-cost fabrication process bridging academic lab research to commercialized production," *Micromachines (Basel),* vol. 7, no. 12, p. 225, Dec 2016, doi: 10.3390/mi7120225.

[70] J. Zhou, D. A. Khodakov, A. V. Ellis, and N. H. Voelcker, "Surface modification for PDMS-based microfluidic devices," *Electrophoresis,* vol. 33, no. 1, pp. 89-104, Jan 2012, doi: 10.1002/elps.201100482.

[71] J. B. Nielsen, R. L. Hanson, H. M. Almughamsi, C. Pang, T. R. Fish, and A. T. Woolley, "Microfluidics: innovations in materials and their fabrication and functionalization," *Anal. Chem.,* vol. 92, no. 1, pp. 150-168, Jan 2019, doi: 10.1021/acs.analchem.9b04986.

[72] J. C. McDonald *et al.*, "Fabrication of microfluidic systems in poly (dimethylsiloxane)," *Electrophoresis,* vol. 21, no. 1, pp. 27-40, Jan 2000, doi: 10.1002/(SICI)1522-2683(20000101)21:1<27::AID-ELPS27>3.0.CO;2-C.

[73] B. S. Rupal, E. A. Garcia, C. Ayranci, and A. J. Qureshi, "3D printed 3d-microfluidics: Recent developments and design challenges," *J. Integr. Des. Process Sci.,* vol. 22, no. 1, pp. 5-20, Jun 2018, doi: 10.3233/jid-2018-0001.

[74] G. S. Fiorini and D. T. Chiu, "Disposable microfluidic devices: fabrication, function, and application," *Biotechniques,* vol. 38, no. 3, pp. 429-446, Mar 2005, doi: 10.2144/05383RV02.

[75] A. V. Nielsen, M. J. Beauchamp, G. P. Nordin, and A. T. Woolley, "3D Printed Microfluidics," (in eng), *Annu. Rev. Anal. Chem. (Palo Alto Calif),* vol. 13, no. 1, pp. 45-65, Jun 2020, doi: 10.1146/annurev-anchem-091619-102649.

[76] Y. He, Y. Wu, J. z. Fu, Q. Gao, and J. j. Qiu, "Developments of 3D printing microfluidics and applications in chemistry and biology: a review," *Electroanalysis,* vol. 28, no. 8, pp. 1658-1678, Apr 2016, doi: 10.1002/elan.201600043.

[77] N. Feuerer *et al.*, "Macrophage retrieval from 3D biomaterials: A detailed comparison of common dissociation methods," *J. Immunol. Regen. Med.,* vol. 11, p. 100035, Feb 2021, doi: 10.1016/j.regen.2020.100035.

[78] A. Stepanenko and V. Dmitrenko, "HEK293 in cell biology and cancer research: phenotype, karyotype, tumorigenicity, and stress-induced genome-phenotype evolution," *Gene,* vol. 569, no. 2, pp. 182-190, Sep 2015, doi: 10.1016/j.gene.2015.05.065.

[79] J. M. Baust, L. H. Campbell, and J. W. Harbell, "Best practices for cryopreserving, thawing, recovering, and assessing cells," *In Vitro Cell Dev. Biol. Anim.,* vol. 53, no. 10, pp. 855-871, Dec 2017, doi: 10.1007/s11626-017-0201-y.

[80] R. K. Ravindran, F. Tablin, J. H. Crowe, and A. E. Oliver, "Resistance to dehydration damage in HeLa cells correlates with the presence of endogenous heat shock proteins," *Cell Preserv. Technol.,* vol. 3, no. 3, pp. 155-164, Sep 2005, doi: 10.1089/cpt.2005.3.155.

[81] E. V. Mymrikov, M. Daake, B. Richter, M. Haslbeck, and J. Buchner, "The chaperone activity and substrate spectrum of human small heat shock proteins," *J. Biol. Chem.,* vol. 292, no. 2, pp. 672-684, Jan 2017, doi: 10.1074/jbc.M116.760413.

[82] R. J. Murphy, G. Gunasingh, N. K. Haass, and M. J. Simpson, "Growth and adaptation mechanisms of tumour spheroids with time-dependent oxygen availability," *PLoS Comput. Biol.,* vol. 19, no. 1, p. e1010833, Jan 2023, doi: 10.1371/journal.pcbi.1010833.

[83] F. Urciuolo, G. Imparato, and P. Netti, "In vitro strategies for mimicking dynamic cell–ECM reciprocity in 3D culture models," *Front. bioeng. biotechnol.,* vol. 11, p. 1197075, Jun 2023, doi: 10.3389/fbioe.2023.1197075.

[84] R.-Z. Lin, L.-F. Chou, C.-C. M. Chien, and H.-Y. Chang, "Dynamic analysis of hepatoma spheroid formation: roles of E-cadherin and β1-integrin," *Cell Tissue Res.,* vol. 324, no. 3, pp. 411-422, Jun 2006, doi: 10.1007/s00441-005-0148-2.

[85] M. Skog, P. Sivler, I. Steinvall, D. Aili, F. Sjöberg, and M. Elmasry, "The effect of enzymatic digestion on cultured epithelial autografts," *Cell Transplant.,* vol. 28, no. 5, pp. 638-644, May 2019, doi: 10.1177/0963689719833305.

[86] R. I. Freshney, "Basic Principles of Cell Culture," in *Culture of Cells for Tissue Engineering*, G. Vunjak-Novakovic and R. I. Freshney, Eds., New Jersey: Wiley-Liss, 2006, pp. 3-22.